

**QUANTIFICATION AND CORRELATION OF
VISCOSE QUALITY CHARACTERISTICS**

A THESIS

Submitted by

NEHA MEHRA

(R670215024)

In partial fulfillment for the award of the degree of

**MASTER OF TECHNOLOGY IN
CHEMICAL ENGINEERING**

(With Specialization in Process Design Engineering)



DEPARTMENT OF CHEMICAL ENGINEERING

COLLEGE OF ENGINEERING STUDIES

UNIVERSITY OF PETROLEUM AND ENERGY STUDIES

DEHRADUN

APRIL - 2017

CERTIFICATE

This is to certify that the thesis entitled “**QUANTIFICATION AND CORRELATION OF VISCOSE QUALITY CHARACTERISTICS**” submitted by **NEHA MEHRA (R670215024)**, to the University of Petroleum and Energy Studies, for the award of the degree of **MASTER OF TECHNOLOGY** in Chemical Engineering with specialization in Process Design is a bonafide record of project work carried out by her under our supervision. The results embodied in this project review report are based on literature and the research in Pulp and Fibre Innovation Centre, Unit of Grasim Industries, Aditya Birla Science and Technology Center (ABSTC). This data is based on proprietary of ABSTC, and hence only Aditya Birla reserves all rights to patent, publish and present the data.

Dr. Rupesh Khare
Research Scientist
Pulp and Fiber Innovation Center
Grasim Industries
Taloja, Navi Mumbai-410208

Dr. ParichayKumar Das
Distinguished Professor
Department of Chemical Engineering
University of Petroleum and Energy
Studies, Dehradun-248007

Signature of the Head of the Department

Date:

DECLARATION BY THE SCHOLAR

I hereby declare that this submission is my own and that, to the best of my knowledge and belief, it contains no material previously published or written by another person nor material which has been accepted for the award of any other Degree or Diploma of the University or other Institute of Higher learning, except where due acknowledgement has been made in the text.

Student Name: Neha Mehra

Roll Number: R670215024

ACKNOWLEDGEMENT

The work accomplished has been fortified by the intellectual vigor and relentless passion for research of many researchers and scientists working at the Pulp and Fibre Innovation Center of Grasim Industries, Aditya Birla. Nonetheless, my journey towards this research project would not have begun without the initiative of my department at University of Petroleum and Energy Studies, the vision of Distinguished Professor Dr. Santosh K Gupta and other professors and management of both the organizations who turned this opportunity into a possibility. Special thanks to Dr. Uday Aggarwal (President, Grasim Industries) for his periodic and pertinent nudges to progress towards the goal with utmost patience.

My mentor at Aditya Birla, Dr. Rupesh Khare's (Research Scientist, Aditya Birla) encouragement towards the approach of learning with experimentation melded with his experience on the process and knowledge left no room for slowdowns. I owe gratitude to Dr. Sagar Deshpande (Research Scientist, Aditya Birla) who endorsed the commencement of the project with MATLAB and bridged the gap for every next move in the project. His exemplary guidance, monitoring and enthusiasm have helped me at every step throughout. The monthly updates and appraisals of project reports by the distinguished professor, Dr. Parichay K Das as my academic guide led to accelerated convergence. He has always inspired and boosted up my confidence.

I would like to thank Mr. Saurabh Singh (FRC, Gujarat) for his guidance, Mrs. Vinaya Godake, Ms. Bhavya Goyal, Mr. Manzoor Shaikh, Mr. Sangram Sonawane and other researchers in the viscose team for their unfledging support. Mr. Vishvas Naik's (Corporate R&D, Aditya Birla) also supported the microscope and image capturing related part of this project. I also laud the resources extended to me, the lab accessories and equipment, the library and computing facilities. Indispensable motivation by my family, my caretaker and my friends has cherished me to conclude this thesis.

Dated: 15th March, 2017

(Neha Mehra)

Place: Dehradun

ABSTRACT

The viscose solutions contain the dissolved cellulose and the undissolved parts in form of undissolved fibres, micro gels, macro gels and the inorganic impurities. These particles influence processing properties of viscose such as filterability and viscosity which lead to industrial problem of clogging of spinneret and breakage of elementary fibres during spinning.

The differences in the quality of the pulp and alkali cellulose or an electron beam treatment have a preferential influence on the macro gel particle content, the micro gel particle content is influenced more strongly by the viscose dissolution temperature and composition of viscose dope. When preparing a viscose it is important to add, at a suitable point in the process, an agent which improves the filterability of the viscose solution. Improved filterability is obtained by the ability of the agent to reduce the formation of gel particles in the viscose solution. As an additional effect, certain, especially suitable agents provide fibres or films with less milkiness and higher brightness.

In order to improve filterability of viscose and minimize the impact of gel content on spinnability and fibre quality experimental studies were carried out. The work done for gel quantification and particle analysis in viscose dope has been directed towards finding the better of the two techniques available namely, first being microscopy using slides containing a drop of viscose and other being microscopy using flow cell (a cuboidal shaped glass tube for viscose to flow in, designed by ABSTC).

The formulation of MATLAB code to detect the particles in images has been done with the help of ImageJ, so as to understand the image processing techniques available and getting the intuition of which technique will work out the best for images take at Aditya Birla. The task to separate out fibres using a code appears challenging. The out of focus images and the non- uniform illumination reduce the devised code's accuracy. Inch by inch progress has been made to reach the proposed objective of quantifying impurities (gels, undissolved fibres and black particles) in viscose dope and to correlate the distribution with the filterability values. The code is expected to provide particle size

distribution of viscose thus segmenting out the gels, undissolved fibres, black particles separately. Aspect ratio, area and geometrical information about particles is the basis for the same using K-means color clustering for RGB images, smoothening followed by gradient on grayscale and HSV images. Along with that an interplay of various other methodologies the quantification protocol has been achieved.

The correlation between particle size distribution and filterability values has been investigated. The classical as well as modern filtration theory have been applied to estimate a filtration value using particles size statistics from code and actual filterability, also called the clogging value or the KW values. The correlation between the two is the ultimate approach towards completion of the set target.

The correlations obtained from image analysis to KW values is weak. The power law fitting to KW values with cumulative total volume distributions per mL from image analysis gives R-square of 0.255. Cumulative volume per mL from Beckman Coulter shows a better correlation to KW values with R-square of 0.61-0.65. However, the polynomial fit to volume distributions per mL from imaging gives R-square of 0.45-0.61. The logarithmic fit to cumulative fibre volume distribution per mL from imaging gives a fit of 0.36 R-square. The image analysis procedure needs to be made robust to count even the translucent gels and swollen fibres with the viscose flow regulated at a constant velocity for all the batches analyzed. The improvements in this direction can be valuable for studying effect of process changes on each segment of impurities separately.

CONTENTS

ABSTRACT		i
CONTENTS		iii
LIST OF TABLES		vi
LIST OF FIGURES		vii
NOMENCLATURE		ix
1	INTRODUCTION	1
1.1)	Cellulose: The basic raw material	1
1.2)	Process Description	1
1.2.1)	Steeping	1
1.2.2)	Pressing	1
1.2.3)	Shredding	2
1.2.4)	Mercerizing	2
1.2.5)	Xanthation	2
1.2.6)	Dissolution	2
1.2.7)	Ripening/Viscose ageing	2
1.2.8)	Filtration	2
1.2.9)	Deaeration	3
1.2.10)	Spinning	3
1.2.11)	Stretching	3
2	LITERATURE REVIEW	7
3	INTRODUCTION TO IMAGE ANALYSIS	12
3.1)	Image Representation Formats	12
3.1.1)	Bits per Pixels (BPP)	12
3.1.2)	Grayscale	13
3.1.3)	Image Types	13
3.1.3.a)	Bilevel	13
3.1.3.b)	Gray 8	13

3.1.3.c) Gray 12	13
3.1.3.d) Gray 16	13
3.1.3.e) Palette	13
3.1.3.f) RGB Color	13
3.1.3.g) Floating point	14
3.1.4) Image Formats	14
3.1.5) Color Models	14
3.1.5.a) RGB Color Model	14
3.1.5.b) HSI(Hue, Saturation and Intensity) and HSV(Hue,Saturation,Value)	14
Color Models	
3.2) K-means Clustering Algorithm	15
4 MATERIALS AND METHODOLOGY	16
4.1) Analytical Techniques Used	16
4.1.1) Clogging Value / Filterability	16
4.1.2) Viscosity Estimation	16
4.1.3) Particle Counts	17
4.1.4) Microscopy - cum- Imaging	17
4.2) Experimentation and Methodologies Devised	18
4.2.1) Trials with Dyes	18
4.2.1.1) Single Dye Trials	19
4.2.1.2) Differential Staining Trials	19
4.2.2) Image Analysis on Softwares	19
4.2.2.1) IMAGE J	19
4.2.2.2) Improsight	20
4.2.2.3) MATLAB	21
4.3) Image Processing Techniques and Parameters in MATLAB	21
4.3.1) The MATLAB Code	22
4.3.1.1) Algorithm to process the Original Image into Separate Images for Fibres, Gels and Black Particles	22
4.3.2) Setting Particle Size Distribution Chart	22
4.3.2.a) Calibration	22

4.3.2.b) Image Counts	23
4.3.2.c) Black Particles	23
4.3.2.d) Gels	23
4.3.2.e) Fibres	26
4.4) Correlating Particle Size Distribution and KW	28
4.4.1) Constant Pressure Filtration	28
4.4.2) KW from Image Analysis	29
4.4.2.1) Methodology	30
4.4.2.2) The Iteration Loop	31
4.4.2.3) Finding the KW and CKW	31
4.5) SOP: Dying, Imaging and Analysis	32
5 RESULTS AND DISCUSSIONS	34
5.1) The Final Code Results for an Image	34
5.2) Reproducibility Study of Image Analysis Code	35
5.3) Effect of bed thickness on calculated KW values	37
5.4) Effect of bed porosity on calculated KW values	38
5.5) Particle distributions from Image Analysis and KW	38
5.6) Correlations of particle size distributions with KW	39
5.7) Particle size distributions from Beckman and KW	46
5.8) A comparison of unaccounted information in Beckman with Imaging	47
6 CONCLUSIONS	50
REFERENCE	52

LIST OF TABLES

Table No.	Description	Page No.
1.1	Viscose Manufacturing	4
2.1	Classification of Undissolved Particles in Viscose	8
3.1	K-means Clustering	15
4.1	Trial runs with Congo Red	20
4.2	Images of dopes using both dyes (Differential Staining)	21
4.3	Critical Imaging Parameters	23
4.4	Particle Separation Techniques and Criteria used in MATLAB Code	24
4.5	The role of gradient and smoothing in Fibre Segmentation	25
4.6	Fibre Segmentation with Sobel filter, Thresholding and Overlap Issue	26
5.1	Final code results in stepwise manner for fibres, gels and black particles	34
5.2	KW calculations from Image Analysis	35
5.7	Viscose Batch Details	47

LIST OF FIGURES

Figure No.	Description	Page No.
4.1	Algorithm to get structural properties for Fibres, Gels and Black Particles	27
5.1	The reproducibility check for volume distribution of gels and black particles	36
5.2	The reproducibility check for volume distribution of Fibres	36
5.3	Calculated KW and KW variations with filter bed thickness	37
5.4	Calculated KW and KW variations with filter bed Porosity	38
5.5.1	Cumulative Volume Distributions for fibres and black particles for batches with different KW values	40
5.5.2	Cumulative Number Distributions for fibres and black particles for batches with different KW values	41
5.6.1	The correlation of KW with Total Particle Volume/mL from Image Analysis	43
5.6.2	The correlation of KW with Total Particle Volume/mL from Image Analysis with one more data point addition	43
5.6.3	The correlation of KW with Total Particle Volume (Total_Vol), sum of Fibre and Gel Volume (Vol_F_G), Black Particle Volume (Vol_BP) from Image Analysis	44
5.6.4	Modified correlation of KW with Total Particle Volume (Total_Vol), sum of Fibre and Gel Volume (Vol_F_G), Black Particle Volume (Vol_BP) from Image Analysis	45
5.7.1	The correlation of KW with Cumulative Volume ($\mu\text{m}^3/\text{mL}$)	45

	from Beckman Coulter	
5.7.2	Particle Size Distribution from Beckman Coulter for 1% viscose sample	46
5.8.1	Particle Size Distribution from Beckman Coulter for 1% viscose sample for comparison to Imaging Results	48
5.8.2	Black Particle Distribution from Imaging for comparison to Beckman Results	48
5.8.3	Fibre Distribution from Imaging for comparison to Beckman Results	49

NOMENCLATURE

A	Total Area of cross-section of filter cake
A _f	Projected Area of Fibre
BF	Ball Fall time in seconds
BPP	Bits Per Pixel
c _k	Cluster centre
CKW	Corrected Filterability Value
d	Euclidean distance between pixel and cluster centre
DP	Degree of Polymerization
D _f	Fibre Diameter
ρ ₁	Density of steel ball in g/cc
ρ ₂	Density of viscose in g/cc
e	Voidage
g	Acceleration due to gravity
KW	Filtration value/ Clogging value
L	Cake thickness
L _f	Fibre Length
η	Coefficient of viscosity in poise
ΔP	Applied Pressure Difference
p(x,y)	Pixel notation for position coordinates (x,y)
P	Fibre Perimeter
t	Time
R	Resistance of the filter bed at time t
r _s	Radius of steel ball in cm
S	Specific Surface area of particles
\bar{u}	Velocity in cm/sec
ú	Volume of Cake deposited per unit volume of filtrate
V	Volume of filtrate that has passes in time t
W	Weight of viscose
μ	Viscosity of filtrate in Poise

CHAPTER 1

INTRODUCTION

1.1) CELLULOSE: THE BASIC RAW MATERIAL

Cellulose, found in plant walls, is the most abundant raw material on the earth. Millions of tons of this bio-renewable polymer are produced every year. Cellulose is capable of producing a number of fibrous products with excellent properties whose utility extends into numerous end uses and industries. Cellulose is an excellent source of textile fibers, for both the commodity and the high-end, fashion-oriented markets. Cellulose does not melt and does not dissolve readily in ordinarily available solvents because of the strong intermolecular bonds. To dissolve the cellulose and to utilize it for fiber making, the viscose making process was developed. In this process, cellulose was converted into sodium cellulose xanthate (through series of chemical and physical reactions using NaOH and CS₂), which was soluble in a caustic solution, making it possible to wet-spin the polymer into a fiber or film. Present report summarizes the objective and learning achieved as a part of internship at Pulp and Fiber Innovation Center (PFIC), Taloja of Grasim Industries Ltd

1.2) PROCESS DESCRIPTION

The viscose process:

Viscose process is a process which is used to convert the natural cellulose occurring in trees into rayon fibres. There are various steps in this processing.

1.2.1) Steeping:

The process converts the cellulose to its alkoxide derivative (alkcell) as the pulp is added to a vigorously agitated tank of lye (17-19%). The pulp swells up and disintegrates into small parts. The temperature for the steeping is kept around 45-55 degree C with the residence time of around 20 min.

1.2.2) Pressing:

The slurry from agitator is then pressed 3-4 times for the removal of excess soda hydraulically at over 120 bars of pressure. This removes all the excess soda present in the

slurry to flow out of the filter plate. This lye is sent back for recirculation and can be used again after makeup.

1.2.3) Shredding:

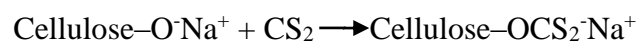
The alkcell in form of cake has a composition of 30–36 % cellulose and 13–17 % soda is broken into relatively dense crumbs. Shredding is usually performed at this stage to open up the alkcell and facilitate the penetration of oxygen during mercerizing and CS₂ into the alkcell.

1.2.4) Mercerizing:

Here, the received pulp typically with a Degree of Polymerization (DP) of 750–850 is reduced to the point at which viscose dope will have acceptable viscosity enough to achieve optimal fibre tensile properties. For regular staple production, the DP of the alkcell going to xanthation needs to be around 270–350. Typical mercerizing time ranges from 0.5–5 hours at temperatures of 40–60 °C.

1.2.5) Xanthation:

The mercerized alkcell is reacted with CS₂ vapor under vacuum to produce sodium cellulose xanthate, ester derivative soluble in dilute caustic soda to form viscose dope. The time for complete xanthation depends on temperature and target CS₂ level, and typically lies between 0.5 and 1.5 hours. Xanthation vessels are often jacketed to ensure constant temperature (25–37 °C). Sodium cellulose xanthate formation occurs as follows:



1.2.6) Dissolution:

Xanthate cellulose is dissolved in dilute sodium hydroxide solution to give the final target viscose composition in terms of percentage cellulose and soda in viscose. Temperature plays a vital role in this process. Low temperatures are better, as the xanthate has greater solubility in NaOH at lower temperatures (0–5 °C).

1.2.7) Ripening/Viscose ageing:

Viscose dope is aged before spinning to allow for the distribution of CS₂ evenly on the cellulose chains which are vital for smooth spinning and good fibre properties.

1.2.8) Filtration:

Regardless of how well the xanthate is brought into solution, there will always be particulate material greater than 15 micron in the viscose that needs to be substantially removed prior to spinning to prevent blockage of the holes in the spinning jet. To filter

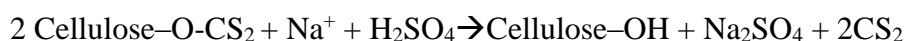
the dope plate and frame filter press is used that is operated at around 3 to 4 bar. Apart from the plate screen, filter cloth is also employed for the process. Care is taken to keep the filtrate cool to avoid degradation of the dope.

1.2.9) Deaeration:

Viscose is deaerated in a stirring vessel while vacuum is applied to remove dispersed air or other gases that might otherwise cause small bubbles to form as the viscose is extruded into filament through the jet. This increases the surface to volume ratio and helps in deaeration.

1.2.10) Spinning:

The sequence of physical and chemical transformations taking place at spinning in spin bath is complex. The main reaction is reformation of cellulose from sodium cellulose xanthate by the action of sulphuric acid.



Sodium salt provides a chemical potential for the water present in the cellulose to flow out and gives fibre of better strength. The zinc forms zinc cellulose xanthate with the dope that enhances the crystallinity of the fibre to give better the tensile property and helps in skin effect to fibre which is very important for dye retention. Between the formation of the zinc complex and the zinc protective layer, the acid penetrates into the fibre causing its regeneration and gives the fibre its primary structure.

1.2.11) Stretching:

The fibre filaments must be stretched over rollers at a slower speed than the final traction units during or very soon after extrusion the filaments. Some stretch is also applied in the spin bath where a significant speed differential exists between extrusion velocity and take-up speed at the godet. Stretching helps in the orientation of the crystalline structure of the fibre. A better oriented fibre has higher tenacity.

Table 1.1: Viscose Manufacturing

PROCESS	REACTANT/ INPUT	PRODUCTS/ OUTPUT	CHEMICAL CHANGE	PHYSICAL CHANGE
<i>Steeping</i>	Cellulose from Pulp NaOH Solution (Lye of 18%(w/w))	Alkali Cellulose (slurry)	Alkali cellulose complex exists in equilibrium with the sodium hydroxide lye Hemi-cellulose and short chained cellulose get dissolved Cellulose I conversion to more reactive cellulose II	Swelling but no dissolution of pulp The pulp gets broken down into smaller fragments
<i>Pressing</i>	Alkali cellulose (slurry)	Alkali cellulose cake	Most of the hemicellulose gets removed with the filtered lye	Weight of the cake formed is measured to get press factor Press factor = weight of cake (g) / weight of dry cellulose (g)
<i>Steeping & Ageing/ Mercerizing</i>	Alkali Cellulose Cake Additives (if required)	The shredded crumbs of alkali cellulose	Oxidative de-polymerisation of the alkali cellulose Homogeneous reaction, catalyzed by heavy metal ions (mainly cobalt or manganese), peroxides play an important role Average cellulose DP of 250-300 is achieved	The cake appears softened

<i>Xanthation</i>	<p>Carbon disulphide (the derivatisating agent) Aged Alkali Cellulose crumbs</p>	<p>Cellulose Xanthate (a soluble compound or ester)</p>	<p>The alkali cellulose reacts like an alcoholate with the carbon disulphide All three OH-groups of the cellulose molecule are involved in the substitution process Formation of more stable C6 derivative</p>	<p>The color of crumbs changes from white to yellow.</p>
Dissolution and Ripening	<p>Cellulose Xanthate crumbs Weak solution of caustic (1-3%)</p>	<p>Viscose Dope that is dissolved cellulose xanthate</p>	<p>The xanthate substituent reduces hydrogen bonding and forces the cellulose chains apart in water for dissolution The ripening process involves a suitable reduction in the number of xanthate groups per glucose unit. The free xanthated groups react with other chains to increase the solubility</p>	<p>The solid crumbs dissolve to form viscous liquid called viscose dope having lower DP.</p>
<i>Filtration and Deaeration</i>	<p>Viscose solution with undissolved particles and air bubbles</p>	<p>Viscose solution with lesser impurities and removed knots.</p>	<p>The ripening of viscose continues while deaeration and filtration</p>	<p>Lesser air bubbles</p>

<p><i>Spinning & Stretching</i></p>	<p>A solution of H₂SO₄, Na₂SO₄ and Zn²⁺ Viscose dope</p>	<p>Regenerated Cellulose Fibre</p>	<p>Xanthate cellulose complex is decomposed immediately when exposed to the bath</p> <p>Zinc ions form a complex with xanthate groups causing cellulose to release one CS₂ per regenerated OH group followed by formation of protective shell by zinc around the xanthate cellulose made of ZnS₂ and Zn(OH)₂</p>	<p>Viscose solution to solid elongated fibre</p> <p>Stretched in order to orient along the fibre axis and goget speeds and inclinations play an important role.</p>
--	---	--	--	--

CHAPTER 2

LITERATURE REVIEW

The debate over the state of viscose dates to 1950s. Treiber (Treiber, 1961) pointed out correctly that the state of technical viscose cannot be described unambiguously and thus theoretical treatment is difficult. The results of experimental studies have supported the presence of gel particles as proposed by Hermans and also the presence of fibrils as pointed out by Dolmetsch. Treiber mentioned that apart from them a large number of otherwise invisible particles were also detected with Zsigmondy ultramicroscope. The results of light scattering measurements of viscose cannot be said to error free due to presence of undispersed particles. Parks et. al. (L.R. Parks, 1960) used electric Coulter Counter for studying particles in the range of 2-15 microns and suggested the use of electric counter over light microscopy as the light microscopy would be difficult in viscose dope with the particles below 15 microns range due to small difference in refractive index between particles (mainly undissolved fibres and gels) and the viscose solution. The working hypothesis used in the paper was that viscose solution is a continuum of particles of all possible dimensions, where the cellulose substance distributes itself in this spectrum according to Gaussian distribution with maximum in the molecular region and the undissolved microscopic fragments in viscose were only a small part of that (E. Treiber, 1963). However, while studying the filterability of viscose in relation to particle size spectrum (L.R. Parks, 1960) placed the real importance on particle range of 2-15 micron as this range usually escapes from the filter media and leads to plugging of spinnerets due to coincident passage and thus weaves into a yarn having potential weak spots and wedge like areas with more frequent breakages. Parks and henceforth, many other researchers carried out their experiments with the electric coulter counter and verified their use for further studies of particle size determinations in viscose.

Broadly, the viscose quality determination methods can be divided into direct methods and indirect methods. The microscopic examination, transparency determination, optical and conductometric determination of gels constitute direct methods while analyzing clogging value and filtration rate through filtration come under indirect method (D.N Arkhangelskii, 1973). The analytical methods for detection of particles and aggregates

were classified as shown in table 2.1 (H. Schleicher, 1998). The quality of viscose or viscose purity is mainly determined by the filtration process. These methods do not permit the location of sources of viscose impurity or regulation of technical parameters of viscose preparation process.

Table 2.1: Classification of Undissolved Particles in Viscose

S. No.	Type of Particle	Analytical Method
1.	Macro gels (Microscopic Region)	Clogging Value/ Filterability Particle Counter
2.	Micro Gels (Sub Microscopic region)	Turbidity Rheology
3.	Chain Aggregates	Light Scattering

These studies are of utmost importance as the purity of viscose determines the quality of fibre produced. A viscose with contaminants and impurities of either undissolved fibres, gels or other inorganic particles is not industrially desired. A large part of literature carries detailed studies about gel particles as impurities rather than fibres and inorganic particles. The focus on gels is pertinent as they are easily deformed, can penetrate through the filter medium and tend to agglomerate also. The chemical composition of gels found in viscose made from different pulps investigated using electron microscopy, X-ray analysis showed that in viscose prepared from wood pulps the gels were primarily composed of cellulose II while in viscose prepared from cotton linters the gels was primarily Xylan (Sperling, 1963). Brandt and Strasser (K. Brandt, 2004) highlighted that gel particles may have different properties. Gels vary from having a rubbery consistency to the ones in fluid state and still having higher viscosity than the surrounding fluid. They emphasized the gel formation mechanism in two ways. First, when dissolving a solid the gel phase is always an intermediate step in the transition of the aggregate condition from solid to liquid. If the time, stirring energy, temperature or shearing force is not sufficient, the gel particles will stay behind in the liquid. Second, the inhomogeneities in the raw material or the crosslinking (high DP of pulp) the conversion of cellulose to alkali cellulose may lead to poor swelling at some localized parts of slurry and serving as sites for gel formation later. Rykova et al. (L.A.Rykova, 1991) also classified gels as primary gels and secondary gels.

The primary gel content, he suggested, is controlled by technical parameters in process of viscose dope preparation while on the other hand the mechanism of generation of secondary gels is traced to polymer residue on solid surface of the equipment and pipelines mainly in the immobile laminar layer of viscose next to the wall where it gets dexanthanated and thus gets accumulated in the solution.

Studies have been made to check the effect of parameter changes or operational modifications in viscose process by change in filterability. The coulter counters came to be increasingly used to observe the effect of changes on particle size spectrum at a more fundamental level. Day-to-day variations in viscose get reflected in counts and the trend of lowering of filtration with the increase in number of large particles was not observed in every case and varies with pulp used (L.R. Parks, 1960). Virezub et al. (A. Virezub, 1972) reported the close relation between variation of viscosity of viscose and chemical processes taking place during ripening were related to the gel particle spectrum at 20 °C in which the relative content in primary γ -6 and secondary γ -2,3 xanthate groups was determined spectrophotometrically while number of gels was determined using TuRZG-1 particle coulter by the known procedure. It was observed that in ripening process the minimum viscosity and thus the completion of redistribution of the xanthate groups coincide with the minimum content in gel particles of all sizes and further ripening created non-homogeneity of gels due to saponification of the γ -6 groups. The increased homogeneity of cellulose xanthate also results in increased flexibility of chains, thus decreasing viscosity. At the same time increased mobility of individual molecules and segments accelerates dissolution of small particles and breaking up of larger ones. With the increased ripening hydrogen bonds are formed as more primary OH groups become free thus increasing viscosity, macromolecular aggregations and gel particle content. Rykova et al. (L.A.Rykova, 1991) determined the gel particle content of the viscose using microscopic method and contrast indicator Congo red by manual counting of gels per drop of viscose on slides. The increase in gel particle content was reported to increase to 65 particles from 5 particles after 24 hours with rise of temperature to 40°C from 20 °C with 2.3 fold increase in xanthate decomposition and only 1.3 fold increase in diffusion for every 10 degree rise in temperature. This indicates that despite the increase of reaction temperature the gel formation did not reduce significantly due to low transport by diffusion in immobile layers. The dwell time of polymeric viscose solution in reactors

thus plays critical role which leads to gel formation also in pipelines used for transport of viscose. The further increase of gel content was attributed to the catalytic effect of metallic surface facilitating local coagulation of viscose and secondary gel particles. Serkov et al. (A.A Serkov, 1986) suggested the oxidative degradation of hemicellulose salts with Fe^{2+} , Ca^{2+} , Mg^{2+} , Co^{2+} , Mn^{2+} or Cu^{2+} that are present in minute quantities in starting cellulose, caustic and water can also increase the gel particle content in dissolving cellulose xanthate.

Since the clogging value also called as filtration value or KW value has been widely used as an indirect measure of viscose quality and the squeezing out of gel particles through the filter media or screen have also led to search for better filtration methods and theories that can relate more precisely to the quality of the viscose dope and its particle content desired to be filtered. Schleicher and Borrmeister (H. Schleicher, 1998) recorded that the ratio of filter values of the viscose prepared from high reactivity pulp and bad reactivity pulp differ in the ratio of 1 to 10. They also observed that the electron beam treatment of pulp within the range of 5-10 kGy helped improve the filterability of viscose even after reducing the CS_2 content though a relatively lesser change in rheo value indicated a changed particle spectrum with a lower amount of gels smaller than 5 microns only. But this change was followed different trend for different pulps and concentrations of CS_2 . The depth filtration is claimed to be a better method of gel filtration as the differential pressure is kept low so as to prevent the squeezing of gel and thus exiting the filter media along with using the backwash feature to remove accumulated gel from metal fibre screen (K. Brandt, 2004). A higher porosity of the filter media is also desired so as to operate with a broad range of differential pressures without any pleating of the filter (K. Brandt, 2004). Treiber (Treiber, 1961) gave a valuable insight as he plotted a positive and linear correlation between gel counts and clogging value taking into consideration the variation in filtration values with the porosity of filter cloth, the capillary structure and their length that may cause the deviation from Hermans-Brede law of filtration. The complete mathematical derivation of four laws of filtration taking four values of n as 0,1, 1.5 and 2 in Hermans and Bredee general law given in equation 2.1 to get clogging constants was also studied by Gonsalves (Gonsalves, 1950) in association with the physical phenomenon taking place.

Equation 2.1

$$\frac{d^2t}{dV^2} = \frac{dR}{dV} = KR^n$$

Where, as per Gonsalves, R is inverse of filtration speed at time t. The second differential form of the equation is formulated by Matthes (A.I. Virezub, 1978).

The transportation and capture of solid particles in filtering medium are due to hydrodynamic, gravitational, molecular, Brownian or electrostatic forces (C. Ghidaglia, 1996). Gonsalves also questioned the wide use of these laws as they do not account for structure of filter medium and viscosity of the solution being filtered. However, a more useful derivation of these laws can be seen in work of Katagiri and Iritani (N. Katagiri, 2016) where the standard law and cake filtration law with $n=1.5$ and $n=0$ respectively take into account the fundamental laws of laminar flows in capillary known as Hagen-Poiseulli equation and Darcy's law and thus modified to get the laws for filtrate of non-newtonian fluids. Iritani derived the filtration laws using Kozeny-Carman equation by considering the variations of porosity and surface area of filter membrane caused by particle deposition.

Hitherto, the undissolved particles in the viscose dope have not been studied separately. Undissolved fibre fragments also affect the filterability adversely but have not been looked into. Image analysis for imaging of viscose dope under microscope has never been used to get particle size distribution. The diameter of the particles in viscose that are captured in images is in order of micrometers and ensure that electrostatic, Brownian and molecular forces are negligible compared to hydrodynamic and gravitational effects during filtration. Hence, the work in this thesis is carried to explore that field.

CHAPTER 3

INTRODUCTION TO IMAGE ANALYSIS

A digital image consists of an array of small elements or picture points referred to as pixels. The position of each pixel is identified by referring it using the rows(x) and columns(y) values. The value of each pixel is a number and it represents the brightness or color of the pixel at that point. The width and height of pixels specify the image's spatial resolution. Once the image is in digital form it can be used to extract a variety of quantitative information. The image processing and analysis process can be categorized as follows:

1) Image processing :

- a) Image Enhancement: The purpose is to make the image clearer for quantitative information extraction. Image contrast, filtering etc. are some of these operations.
- b) Image Restoration: It is done to restore image from a distorted, blurred or warped image.

2) Image Analysis:

- a) Image Feature Extraction: Image is transformed or operated so that certain features and objects can be identified and extracted.
- b) Image Measurements: It is done to extract meaningful data from the image so as to use it for detection of objects and features, size and shape measurements of features, determining position of objects, measurements of intensity or optical densities and description of scenes.

3.1 IMAGE REPRESENTATION FORMATS

3.1.1 BITS PER PIXEL (BPP): when a digital image is acquired through a device such as a CCD camera or a scanner, the brightness/color at each pixel location is first detected and stored as a number at the location of pixels in the array. The number is in binary format that is a string of bits (1 or 0). The number of bits used to represent and store the value of pixel is known as Bits per Pixel (BPP) or Pixel Depth. This

value is set depending upon image acquisition software used and as per the utility of the user.

3.1.2) GRAYSCALE: It is an monochrome image (where the value of a pixel denotes the brightness of the pixel at that point in the image) where the range of color is between black to white. The gray scale range of the image is the possible range of values used to represent the brightness. A completely black pixel has value 0. The upper limit of brightness depends on bits per pixel used in the image. Usually a common gray scale image has range from 0 (black) to 255(white) with other shades occupying intermediate values.

3.1.3) IMAGE TYPES: Depending on BPP, digital images can be of different types and formats as below:

3.1.3.a) Bilevel: Uses 1 BPP for storage.

3.1.3.b) Gray 8: A monochrome image with grayscale range from 0 to 255 (or 256 gray levels). Uses 8BPP. Most widely compatible with hardware devices.

3.1.3.c) Gray 12: A monochrome image with grayscale range from 0 to 4095. Uses 12 BPP. It is generated by specialized type of hardware.

3.1.3.d) Gray 16: A monochrome image with grayscale range from 0 to 6535 using 16 BPP.

3.1.3.e) Palette: It is a color image using 8BPP for storage. Maximum number of colors that can be depicted in the image is 256. A list of values for the palette of colors used in the image is stored along with the image. The value of each pixel is an index to an entry in this list. Palette format reduces the memory needed to store a color image than has fewer than 256 colors. It is convertible to Gray 8 or RGB color before analysis operation.

3.1.3.f) RGB Color: A true color using 24 BPP. The values for primary colors Red, Green and Blue (RGB) are stored separately for each pixel and each color uses 8 bits to represent the brightness of that color (0 to 255). When the final

image is displayed, the three primary colors are combined to obtain the final color of the pixel using mathematical relation.

3.1.3.g) Floating Point: It uses 32 BPP. The image is usually created from gray scale or color image. The advantage of this format is that it is the processing operations that generates integer values irrespective of others which generate negative, fractional or large values making it useful in certain image enhancements and restorations.

3.1.4) IMAGE FORMATS: The file size of images vary with their Resolution (the total number of pixels used to represent the image) and also their pixel depth. Greater the number of pixels greater the BPP, larger the file. Based on the compression method, various file formats are obtained such as BMP, JPG, GIF etc.

3.1.5) COLOR MODELS: It is a mathematical model representing the way in which color is described. RGB, HIS and HSV color models use three vectors and each point located anywhere on these vectors represents the unique value used to make the image.

3.1.5.a) RGB Color Model: an additive color model using primary colors of red, green and blue in different proportions to produce a wide range of colors. White is produced by combining the pure color (the highest value) of red, green and blue in equal quantities. And absence of all the three colors result in black.

3.1.5.b) HSI (Hue, Saturation and Intensity) and HSV (Hue, Saturation, Value) Color Models: These are better representation of color relationships and combinations. When we speak of different colors we actually talk about Hue. Hue differs from color as color can have saturation and brightness along with hue. Saturation represents how pure the color is that is the strength of the color. It is the intensity of a hue from gray scale (no saturation) to pure color(high saturation). Brightness is relative expression of lightness or darkness of a particular color, from black (no brightness) to white (full brightness). It is expressed as intensity or value.

3.2 K-MEANS CLUSTERING ALGORITHM

N. Dhanachandra et al. (N. Dhanachandra, 2015) explained the algorithm for an image with resolution of $x \times y$ and has to be cluster into k number of cluster. Let $p(x, y)$ be an input pixels to be cluster and c_k be the cluster centers. The algorithm for k -means clustering is following as:

1. Initialize number of cluster k and centre.
2. For each pixel of an image, calculate the Euclidean distance d , between the center and each pixel of an image using the relation given in Table 3.1.
3. Assign all the pixels to the nearest centre based on distance d .
4. After all pixels have been assigned, recalculate new position of the centre using the relation given in Table 3.1.
5. Repeat the process until it satisfies the tolerance or error value.
6. Reshape the cluster pixels into image.

Table 3.1: K-means clustering

Step 2	Step 4
$d = \ p(x, y) - c_k\ $	$c_k = \frac{1}{k} \sum_{y \in c_k} \sum_{x \in c_k} p(x, y)$

Although k -means has the great advantage of being easy to implement but the quality of the final clustering results depends on the arbitrary selection of initial centroid. Computational complexity is another term which we need to consider while designing the K -means clustering. It relies on the number of data elements, number of clusters and number of iteration.

Hence, the understanding on image analysis techniques and algorithms is imperative to extract the information conveyed through images.

CHAPTER 4

MATERIALS AND METHODOLOGY

4.1 ANALYTICAL TECHNIQUES USED

The work undertaken has several sub-stages involved in it:

4.1.1) CLOGGING VALUE / FILTERABILITY

Filter clogging value can be measured either by weighing the discharge quantity of viscose under constant pressure or by the increasing pressure of filtration under constant discharge quantity. We are working under constant pressure of 2.1 kg/cm² and use filter Paper as the filter medium.

General Formula Used:

$$KW = (t_1/W_1 - t_2/W_2) * 2 * 100000 / (t_1 - t_2)$$

Where:

t₁ = 40 minutes, t₂ = 20 minutes

W₁ = Weight of viscose collected in 40 minutes

W₂ = Weight of viscose collected in 20 minutes

Because the viscosity of the viscose influences the clogging value, we correct the determined KW value by the viscosity according to:

$$\text{Corrected KW} = KW (1 + a/100)$$

Where:

a = BF - 55, if 25 < BF < 80 and a = 80 - 55, if BF > 80

BF = Ball fall time in seconds

4.1.2) VISCOSITY ESTIMATION

The viscosity of filtered viscose is measured using Ball Fall method where the steel ball is made to fall between two points marked on the glass tube filled with filtered viscose and time of fall is measured. The working principle is that when a small sphere falls under the action of gravity through a viscose medium it ultimately acquires a constant velocity given by Stokes's Law:

$$\bar{v} = 2 * g * r_s^2 * (\rho_1 - \rho_2) / (9 * \eta_k)$$

Where:

\bar{v} = Velocity in cm/sec

g = acceleration due to gravity

r_s = radius of steel ball in cm

ρ_1 = density of steel ball in g/cc

ρ_2 = density of viscose in g/cc

η_k = Coefficient of viscosity in poise

4.1.3) PARTICLE COUNTS

Additional information about number and size of macro gel particles plus other particles of similar size may be obtained by particle counting in viscose. The various commercial devices for the particle counting are working on different principles, e. g. the difference in electrical conductivity or Optical density between particle and solution. Each method has its advantages and disadvantages. Initially we were using Beckman Coulter for the same but now quantification through Image Analysis is the key focus as B.

4.1.4) MICROSCOPY-cum- IMAGING

Currently the microscopy cum camera imaging is performed on viscose samples collected at three intermediate stages in the process. The viscose collected from dissolver is filtered and collected. The viscose before filtration is called unfiltered viscose and that collected after filtration is called filtered viscose. The reject after filtration is also collected and is called reject viscose.

The imaging is done at 140X resolution and digital images are automatically captured and saved after every 5 seconds using IC Capture (Version 2.3) software as each of the viscose sample is made to flow in a glass cubical tube of 0.5 cm depth, 4cm axial direction length and 1 cm wide.

The depth of focus of the telescopic lens is measured and calculated to be 250 microns at mark 4 or 140X by measuring the change in vertical distance transversed by microscope lens holder in the degree of rotation that makes the object in focus out of focus in both anti-clockwise to clockwise direction from the focused position.

As observed from the images in above table, reject viscose shows more number of un-dissolved fibres as compared to un-filtered and filtered viscose samples. It is possible that such un-dissolved fibres are the reason for clogging of filter resulting in higher filter clogging values (KW).

4.2 EXPERIMENTATION and METHODOLOGIES DEvised

Out of static microscopy on glass slides and the other one being flow cell imaging the latter was found to be more reliable as the quantity of viscose analyzed was more, the factor of external impurities present in slide based analysis were eliminated and time required was also reduced. Then arises the limitation of differentiating the undissolved fibres and gels from the remaining viscose as they possess the Intensity and RGB values that overlap in the same range. The task becomes daunting as we try to go for gradients and other exponential approaches to magnify the irregular and randomly varying intensity differences between the two. Thus, different dyes were put into viscose dope to achieve selective dyeing of the undissolved fibres and gels so as to create a well defined and separate range of RGB values

4.2.1) TRIALS WITH DYES

The dyeing experiments on viscose were carried using four different dyes which are listed below. The dyes selected were initially testing the dyeing of regenerated viscose fibres.

- 1) Violet Dye
- 2) Blue Dye
- 3) Red Dye 1
- 4) Congo Red Dye

4.2.1.1) SINGLE DYE TRIALS

Dyeing solution of three different concentrations i.e. Dilute, Medium and High concentrations were prepared for all four dyes by dissolution in water. Different amounts of each concentration was put and mixed in viscose dope. The dyed dope was analyzed under microscope by transferring a small amount of each dyed viscose in petri dish.

Observations: The relative RGB ranges and contrast could not be magnified to create separate range for the background viscose and undissolved fibres and gels.

4.2.1.2) DIFFERENTIAL STAINING TRIALS

The Congo Red dyed viscose dope was again dyed with the blue dye solution until the red color of the dope changed to greenish brown. The same was done using differently concentrated solutions of both dyes and adding different amounts of them to dope

Observations: The images taken did show a visually differentiable contrast between the two. The gels and undissolved fibres appeared red against the dark, bluish background (Table 4.1 and Table 4.2). During high concentration of Congo red dye used in the differentially dyed viscose, both fibres and gels (both being cellulosic particles) were getting colored. However, the flow cell imaging required the exposure to be increased to such a value that streak effects were arising. Hence, the experiments were done to lowered and optimize the concentration of Congo red dye such that the gels can be colored and fibres can remain uncolored. This made flow cell imaging simple and at decreased exposure values.

4.2.2) IMAGE ANALYSIS ON SOFTWARES

4.2.2.1) Image J: Image J is a free software available for particle analysis. This was employed to enhance contrast, adjust brightness, to sharpen and smoothen the saved images. All these features are built in Image J and a selection of the image processing operation is required by user to process the image, without the use of a code. The Macro feature along with plug-ins is also available to run the software in conjugation with a user-defined code. It was extremely helpful to get the basic guidelines for the advanced image processing code developed later in MATLAB. ImageJ was used to enhance the

contrast of differentially dyed viscose and prepare a magnified intensity difference image for processing it with K- means clustering to get gel particles accurately

4.2.2.2) Improsight: Camera images taken as viscose flows in flow cell were also sent to the host computer where they are analyzed as they arrive. The images after analysis by software are transferred and saved into a target folder .There is no need to wait until all images are captured to begin image processing and data reporting. The time interval for processing images as the viscose flows in the flow cell can be set by user. The software analysis the air bubbles and black particles based on the RGB range set by the user. At the end of a run the accumulated particle statistics are available for display, printing, or export to Microsoft Excel format. This was used briefly to detect black particles but due to some visible errors in counting and limitation to periodically renew the license its working was not so efficient.

Table 4.1: Trial Runs with Congo Red

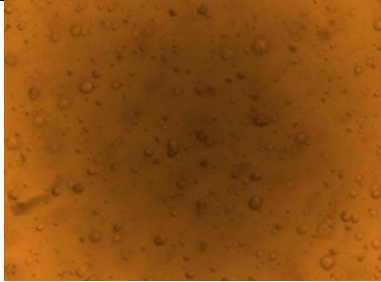
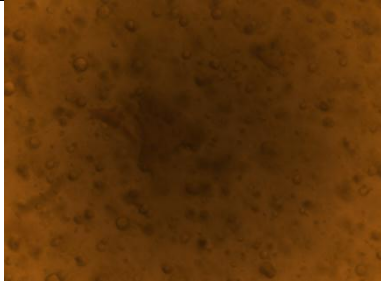
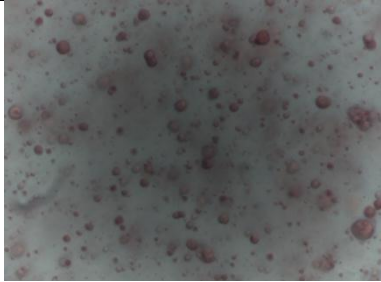
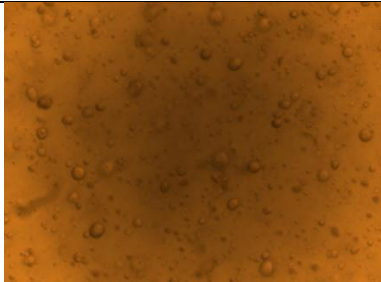
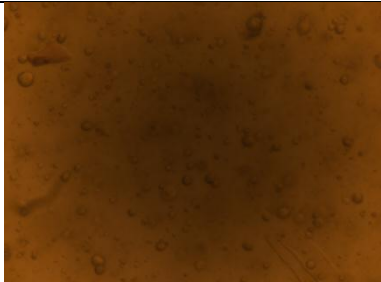
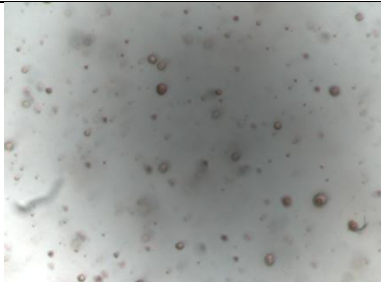
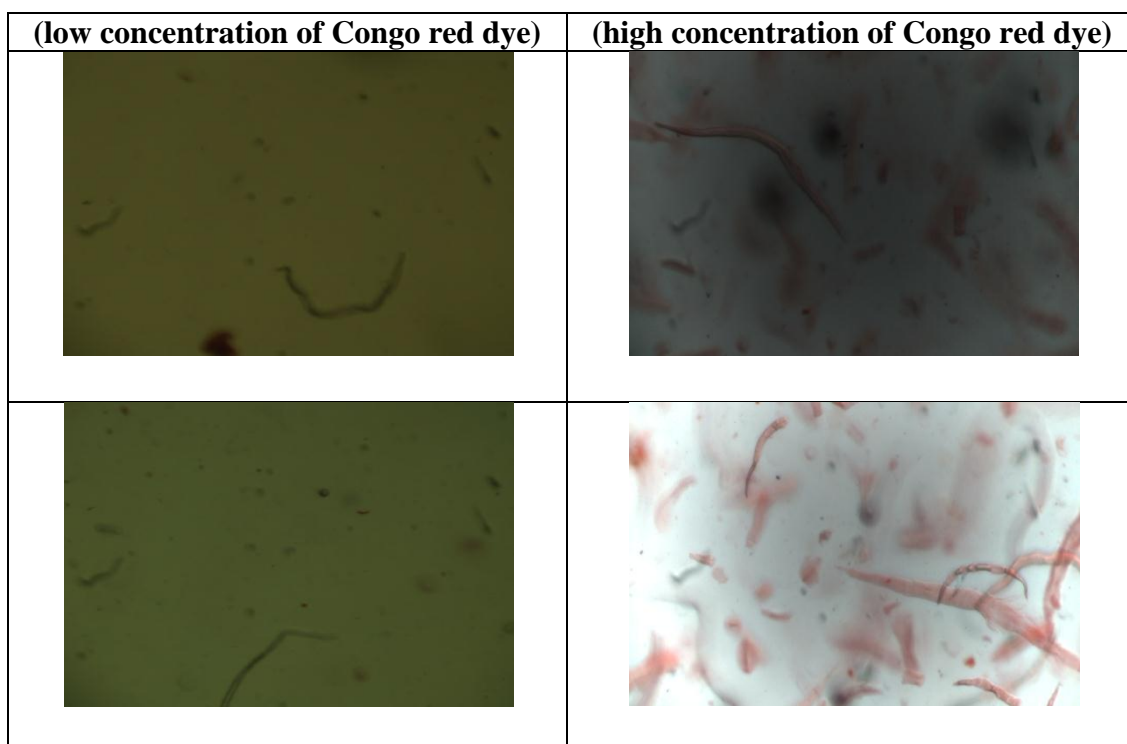
Undyed Viscose	Viscose Dyed with Congo Red	Viscose Dyed with Red and Blue Dyes
		
		

Table 4.2: Images of dopes using both dyes (Differential Staining)

Unfiltered Viscose	Reject Viscose
--------------------	----------------



4.2.2.3) MATLAB: MATLAB is a well-known software used to write specific objective-oriented codes by user as required. The need to write a code arises as the both the above mentioned softwares failed to identify the undissolved fibres and gels. The fine and precise RGB values need to be set to differentiate undissolved fibres and gels from the remaining viscose. This necessitates the development of a reliably accurate and precise coding. Moreover, the use of dyes that in return changed the RGB values and relative contrast between background and objects of focus also require code that incorporates the respective modifications for analysis and quantification.

4.3 Image Processing Techniques and Parameters in MATLAB

The image processing code in MATLAB was formulated after much experimentation with different imaging techniques available in MATLAB. Some of the factors that are paid attention are listed below in Table 4.3 and Table 4.4. The smoothing and gradient techniques played important role in processing of images for segmenting fibres as shown in Table 4.5, while were not required during k-means clustering for red gels. Elimination

of background particles that were visible on all images was important during fibre and black particle detection. The image processing had to proceed sequentially from red gels to fibres to black particles as both fibres and black particle segmentation is based on thresholding as an intermediate step and hence the regions that are occupied by red gels have to be removed prior to segmenting the remaining impurities in images. While images are captured, the multiple fibre overlapping should be avoided as the code formulated will not be able to point out the segmented fibres as fibres due to the aspect ratio that is the final geometric parameter for fibre segmentation as shown in Table 4.6.

4.3.1) THE MATLAB CODE

4.3.1.1) Algorithm to process the original image into separate images for fibres, gels and black particles

The algorithm developed for MATLAB code is shown in Figure 4.1. At the completion of the run over all images in file folder using the devised code at the inbuilt Batch Processing App platform available in MATLAB, the collective result is saved by typing the following command in workspace:

'Save SampleFileName allresults'

Where SampleFileName is decided by user and is usually the batch name of the viscose whose images are analyzed along with the indication of KW values of that batch.

4.3.2) SETTING PARTICLE SIZE DISTRIBUTION CHARTS

As the statistics of particle distribution are obtained then the next step is the processing of results obtained for all the three undissolved particles. This is done in another code devised solely to post process the images whose results are saved as stated above.

4.3.2.a) Calibration: The pixel counts are converted to real dimensions of length i.e. microns to summarize the particle distribution on semi-log charts of particle diameter versus particle count, semi-log charts of particle diameter versus cumulative volume of particles per ml viscose. The calibration scales were verified for magnified images using Image J.

4.3.2.b) Image Counts: The total number of images that were processed for a particular batch using the algorithm of Step 1 are counted to get the total volume of viscose processed by multiplying depth of focus of microscope by the area of the images

captured at the fixed dimensions of 1920* 1080 pixels after calibrating in microns. The volume of sample analyzed per image came out to be $196731 * 10^{-9}$ millilitre.

Table 4.3: Critical Imaging Parameters

Critical Parameter		Fibre	Gel	Black Particle
1.	<i>Non-Uniform Illumination</i>	Yes	No	Yes
	<i>Solution</i>	a) Constant Power Supply b) Smoothing	Not Required	a.1) Constant Power Supply a.2 Select suitable magnification b) Adaptive Thresholding
2.	<i>Impact of Discoloration</i>	Yes	Yes	No
	<i>Solution</i>	a) Using the right concentration of Red Dye	a) If not dyed, then not detected by code b) Neglect pixels with Green (G) value above desired	Not Required
3.	<i>Blurred Edges</i>	Yes	Yes Very Less	Yes Moderate
	<i>Solution</i>	a) Not controllable b) Gradient method	Not required	a) Compensated by internal dark core

**** a= Control applicable during Image Capture, b= Control Applicable In MATLAB Code**

4.3.2.c) Black particle: The equivalent diameter is calculated as four times the ratio of particle's area to its perimeter. The volume, projected surface area and total surface area of particles are calculated using the formulas for spheres.

4.3.2.d) Gels: The equivalent diameter is calculated as for black particles. However, volume, projected surface area (P.S.A) and total surface area (T.S.A) are calculated differently. As observed from images the gels were found to usually 12 microns thick and hence are taken to be a cuboid and not treated spherical in shape.

Thickness of gels= 12 microns

Volume of gels= (P.S.A in 2-D image)*(12 microns)

$$\begin{aligned} \text{T.S.A of Gels} &= (\text{Surface Area of base and top} + \text{Surface Area of lateral surfaces}) \\ &= (2 * \text{P.S.A}) + (\text{Perimeter of Gels from 2-D image} * 12 \text{ microns}) \end{aligned}$$

Table 4.4: Particle Separation Techniques and Criteria used in MATLAB Code

<i>Goal</i>	FIBRES	GELS	BLACK PARTICLES
<i>Separation Technique Used</i>	1) K-means Clustering 2) Geometric Criteria In Binary Image	K-means Clustering	1) Adaptive Thresholding of : a) GrayScale Image b) HSV Image
<i>Physically Perceivable Criteria</i>	1) Color 2) Intensity 3) Shape	1) Color (Red)	1) Color 2) Saturation/ Darkness
<i>Separation Parameter Used in MATLAB Code</i>	Clusters=2 Maximum Mean Cluster Value	Cluster=3 Maximum Mean Cluster Value	1) Threshold Value
<i>Geometric Criteria Used</i>	Aspect Ratio >3 where aspect ratio is $\frac{\text{MajorAxisLength}}{\text{MinorAxisLength}}$	None	None

Table 4.5: The role of gradient and smoothing in Fibre Segmentation

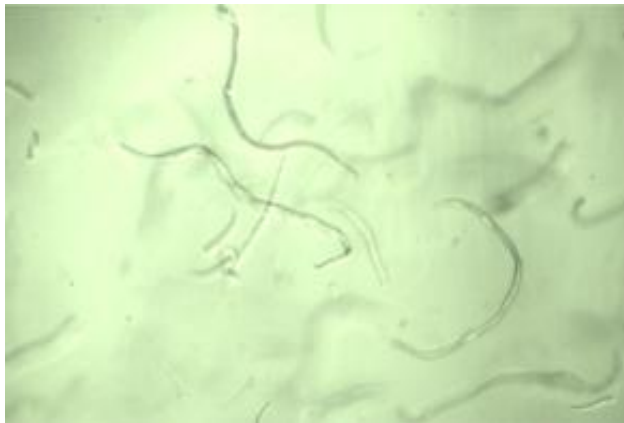

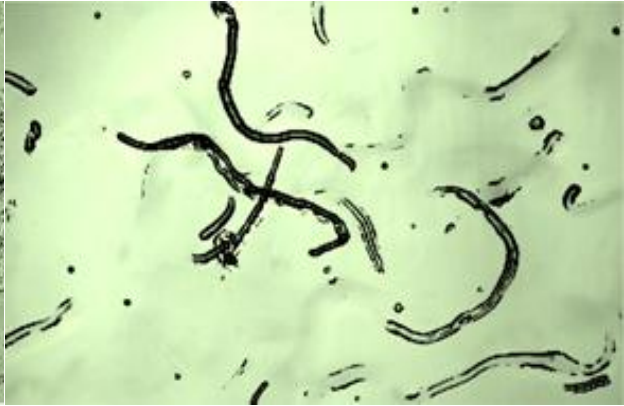

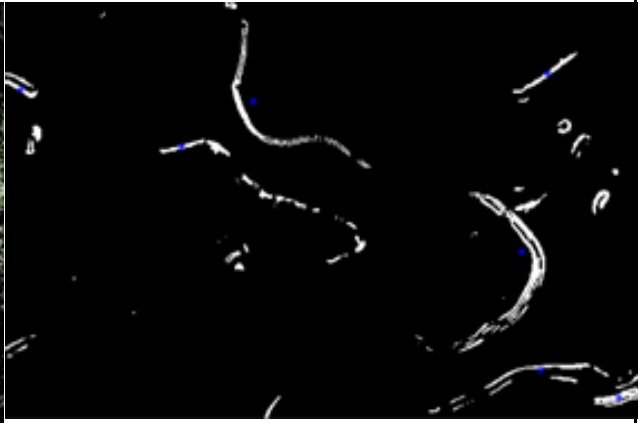
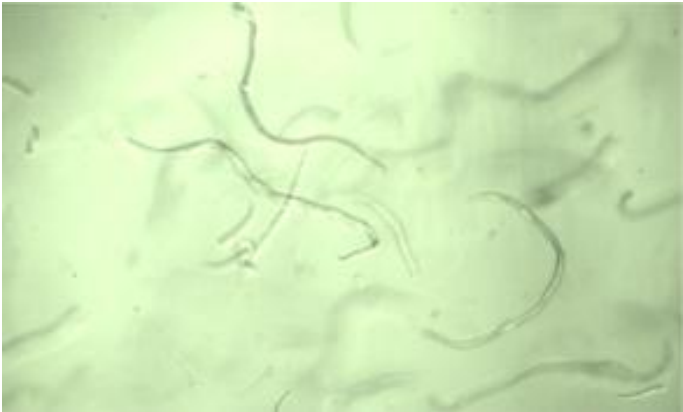

<p>FIBRE SEPARATION</p> <p>(Original Image)</p> <p>METHOD 1: K-means Clustering</p> <p>Clusters=2</p> <p>Fibre Cluster= Maximum Mean Cluster Value</p>	
<p><i>Without Smoothing and Gradient</i></p>	<p><i>With Smoothing and Gradient</i></p>
<p>Cluster1</p> 	<p>Cluster1</p> 
<p>Cluster2</p> 	<p>Cluster2</p> 

Table 4.6: Fibre Segmentation with Sobel filter, Thresholding and Overlap Issue

<p>FIBRE SEPARATION</p> <p>(Original Image)</p> <p>METHOD 2: Geometric Criteria in Binary Image</p> <p>Fibre Aspect Ratio > 3</p>	
<p>The overlapped fibres are not detected as fibres as the centroid for each fibre detected is shown in blue color and is not present for overlapped fibres.</p>	

4.3.2 e) Fibres: The diameter of the fibres as seen in images varied depending upon the state of fibre such as thick or swollen fibre and thin or unswollen fibre. But mostly fibres of an average of 16 micron are present in images at 140 X magnification. Hence, the fibre diameter was used as 16 micron for further calculations.

Though, another criteria can be used to get fibre length and diameter as fibre area and fibre perimeter are known. This criteria works on assumption that all the fibres segmented in image are cylindrical in shape and the projected area on image is thus a rectangle with length as fibre length and breadth as fibre diameter. The quadratic equations can be formed where the sum of roots is negative of half of fibre perimeter

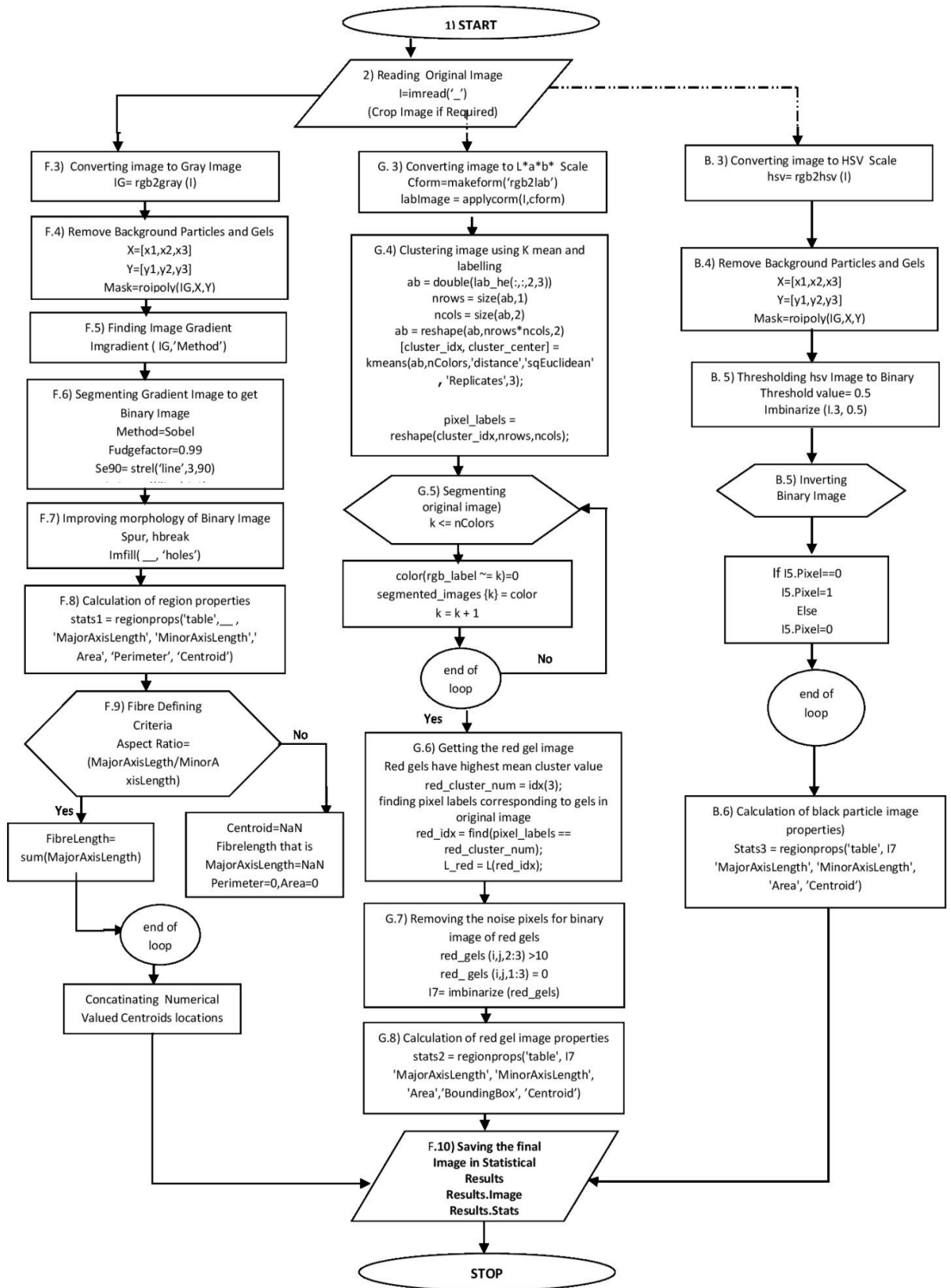


Figure 4.1: Algorithm to get structural properties for Fibres, Gels and Black Particles

and product of roots is the area. The quadratic equation is shown below and can be used to get fibre dimensions.

$$P = \text{Fibre Perimeter} = 2(L_f + D_f)$$

$$Af = \text{P.S.A of Fibre} = L_f * D_f$$

$$x^2 + \left(-\frac{P}{2}\right)x + Af = 0$$

However, both the criterias have their own pros and cons. Overall, the cumulative P.S.A of fibres and cumulative Volume of fibres played the role of varying filterability and hence the user can proceed to use any of the criteria after looking into reproducibility graphs obtained using each of the above.

4.4 CORRELATING PARTICLE SIZE DISTRIBUTION and KW

4.4.1) CONSTANT PRESSURE FILTRATION

From the theory of constant pressure filtration (J. Coulson, 1998) we know that the factors affecting the rate of filtration are:

- a) The pressure drop from the feed to far side of the filter medium
- b) The area of filtering surface
- c) The viscosity of filtrate
- d) The resistance of filter cake
- e) The resistance of filter medium and initial layer of cake

The particles forming the cake are small, flow obtained through the bed is streamlined and slow. It is assumed that cake is uniform and voidage is uniform. But throughout the filtration the voidage depends on the nature of support, including its geometry and surface structure and rate of deposition. The flow rate of filtrate may be represented by following equation:

Equation 4.1:

$$\frac{1}{A} \frac{dV}{dt} = \frac{1}{5} \frac{e * e * e}{(1 - e) * (1 - e)} \frac{-\Delta P}{S * S\mu l}$$

The integration of above equation for constant pressure filtration gives

Equation 4.2:

$$V = \sqrt{\frac{2 * A * A * \Delta P * t}{r * \mu * \dot{v}}}$$

Equation 4.3 gives r as:

$$r = \frac{5 * S * S * (1 - e) * (1 - e)}{e * e * e}$$

\dot{v} = Volume of cake deposited per unit volume of filtrate

V = Volume of filtrate that has passes in time t

A = Total Area of cross-section of filter cake

L = cake thickness

e = Voidage

ΔP = Applied Pressure Difference

μ = Viscosity of filtrate

S = Specific Surface area of particles

4.4.2) KW FROM IMAGE ANALYSIS

The model used to determine filterability from image analysis works on incorporating the change in filter cloth porosity as a function of time and filtrate volume passed in time t .

Thus, the filter cake is assumed to be compressible. The constants terms of *equation 1* are A and ΔP and thickness of filter bed.

Geometry of filter bed:

The geometry of filter bed is constant for all the batches of viscose analyzed. The volume of filter bed with circular cross-section = A *thickness of bed

- $\Delta P = 2.1 \text{ kg/cm}^2$
- Diameter of filter cross-section = 1 cm
- Thickness of Bed = 0.035 mm

Variables dependent upon the Viscose Dope sample analyzed:

- μ (in poise) = $BF * 1.855$
where BF = Ball fall in seconds
- Volume fraction of undissolved particles analogous to \dot{v} .

\tilde{v} = Cumulative Volume of Fibres, Gels and Black Particles per unit volume of Viscose Dope

- $S = \frac{\text{Cumulative Total Surface Area of Fibres, Gels and Black Particles}}{\text{Cumulative Volume of Fibres, Gels and Black Particles}}$
- \tilde{V} = Volume of impurities greater than the filter pore size per unit volume of Viscose Dope
- $R = (1-e)^2 / e^3$

4.4.2.1) Methodology

It is based on assuming e as a function of V and t .

$$e = f(V, t)$$

or

$$V = g(e, t)$$

where modifying equation 4.2 gives V as :

$$V = \sqrt{\frac{2 * A * A * \Delta P * t}{5 * S * S * \mu * \tilde{v} * R}}$$

Defining a constant K as:

$$K = \frac{2 * A * A * \Delta P * 60}{5 * 1.855}$$

Where the time in minutes is converted in seconds using conversion factor of 60 and 1.855 comes from the formula of converting ball fall to viscosity in poise.

Defining another constant VK as:

$$VK = \frac{K * (10^4)}{S * S * \tilde{v} * BF}$$

Therefore,

Equation 4.5 gives V as:

$$V = \sqrt{VK * \frac{t}{R}}$$

4.4.2.2) The Iteration Loop:

Assuming the filter cloth to be 100% efficient the porosity is calculated as follows:

Equation 4.6:

$$e_i = e_{(i-1)} - \frac{\tilde{V} * V_{(i-1)}}{\text{Total Volume of Bed}}$$

Where i =number of iteration

Following iteration loop over a time interval of 40 minutes with a step size of 1 minute is employed in calculating the KW from image analysis:

- a) **Step 1:** Estimate an initial porosity e_0
 Calculate R_0 using formula of R, defined above.
 For $t = 1 \text{ min} = 60 \text{ sec}$
 Use Equation 5 to get V_0
 Use equation 6 to Calculate e_1
- b) **Step2 :** Begin the loop with $t=1$ and run till $t=40$ with the volumes obtained at each iteration being saved as a vector matrix

4.4.2.3) Finding the KW and CKW

At the end of iterations the formula for finding the KW that is employed on measured volumes obtained by multiplying density of viscose (1.12 g/cc) with the mass balance readings obtained at 20 and 40 minutes is used.

From the volume matrix formed above the cumulative volume upto 20 minutes and cumulative volume upto 40 minutes is found and inserted into the formula to get the KW.

Consequently the CKW is also found by the same formula from the KW.

4.5 SOP: DYING, IMAGING AND ANALYSIS

The complete methodology is as stated below:

- 1) Prepare 0.01%(w/w) of Congo Red dye solution and 0.05% (w/w) of Blue dye solution
- 2) Filter both the dye solutions from 0.2 micron filter.
- 3) Take 30 g of viscose samples to be analyzed in a beaker.
- 4) Add 14-15g* of filtered Congo Red dye solution in small amounts of 1 g with constant stirring to mix it well with the viscose.
- 5) Add 25-30g* of Blue dye solution to the above red colored viscose with constant mixing till the red color from the viscose changes to brownish- yellow (If more blue dye is added the color may turn to dark greenish-brown).
- 6) Deaerate the colored viscose dope so to remove entrapped air bubbles.
- 7) Set up the imaging set by placing funnel in the holder at some height.
- 8) Connect the funnel to the cuboidal flowcell by pipe of 15cm length so as to make the viscose flow through it. Attach another pipe of same length at the outlet of flowcell (the end opposite to the funnel side) for viscose to exit.
- 9) Place a container at the other end to collect the input viscose sample.
- 10) Set the microscope at the appropriate magnification of 160X (mark 4) or 180 X (mark4.5).
- 11) Start the IC capture software and make the folder for the images to be saved by set run time settings option under Capture tab from toolbar and also the total time of imaging (10-15 minutes) and time interval (3-5seconds) between consecutive images.
- 12) Set the exposure value between (1/120 to 1/60) so as to capture the images not so bright and not so dark. Set the image type to RGB32(1920*1080) and FPS to the 60 or maximum available value at this dimensions 1920* 1080.
- 13) Add the deaerated viscose to the funnel from a side to prevent air bubbles.
- 14) As the viscose passes through the flowcell start the timer in IC capture software. The software captures the image at specified interval for the time specified in the created folder.
- 15) Once the images are captured start the Image Processing App in MATLAB.

- 16) Load the desired image processing code and then load the images from the folder of the particular batch of viscose.
- 17) Set the threshold value for black particles which may vary from 0.38-0.55 depending on exposure values used for image capture.
- 18) Select the 'Process All' option to process all the loaded images and wait till processed.
- 19) Export the results for Black Particles, Fibres and Gel stats of all images in workspace.
- 20) Save the results by command "save BatchName.mat allresults". (Batch Name is user specified).
- 21) Load Code 2 in MATLAB to arrange the results saved above for 1 batch into equivalent diameters and length (for fibres) bins along with specifying the measured KW, BF, CKW for the batch. Save the results by command "save LA-BatchName.mat T" where T is the table that contains the results for fibres, gels and Black Particles.
- 22) Process different batches using App and code 2 and then load Code 3 in MATLAB. Using Code 3 the results of multiple batches that are saved by name LA-BatchName.mat in a common folder can be analyzed for batch wise comparisons.



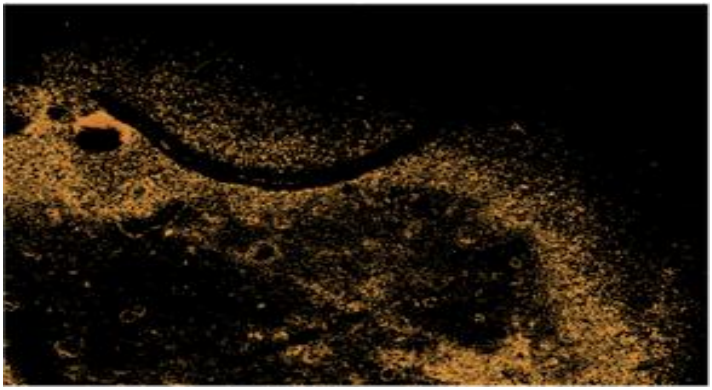
** The amount of dye to be added varies with the amount of viscose taken and is subject to variations to ensure proper coloration of viscose.*


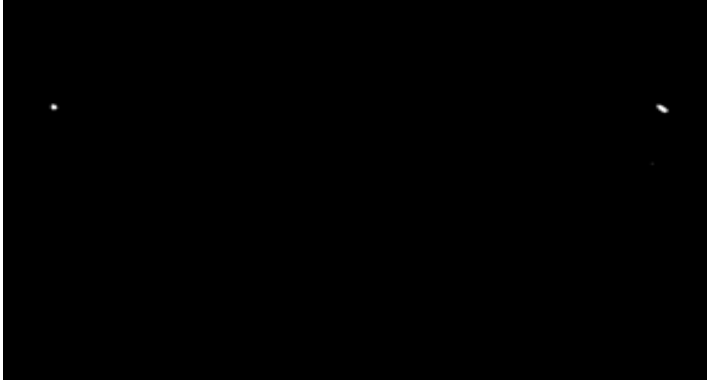
CHAPTER 5

RESULTS AND DISCUSSIONS

5.1 THE FINAL CODE RESULTS FOR AN IMAGE

Table 5.1: Final code results in stepwise manner for fibres, gels and black particles

<p>1) Original Image</p>	
<p>2) Cropping and Background Reduction</p>	
<p>3) Detecting Red Gels (No Red Gels Found)</p>	

<p>4) Detecting Fibre (Centroid Location in blue of fibres detected)</p>	
<p>5) Detected Black Particles (2 Black Particles in white visible in binary image found)</p>	

5.2 REPRODUCIBILITY STUDY OF IMAGE ANALYSIS CODE

The accuracy and the ability of the code formulated is essential to authenticate its use for further analysis. The number of images that need to be processed per sample by the MATLAB code was also a variable and a range of number of images to be processed for establishing particle size distributions and the correlation studies has to be finalized. Hence, the reproducibility of the code was verified. The reproducibility results of one the batches of viscose namely V218 is shown in Figure 5.1 and Figure 5.2 where the number of images processed are 120 and 60 as shown in graphs with notation '120im' and '60im'. The KW value for the batch is 370 and also represented in the legends. The prefix 'LA-' is used as a MATLAB identifier for the command to process results of batches with the prefix 'LA-' and .mat is the MATLAB file format extension.

Table 5.2: KW calculations from Image Analysis

Calculated KW from 120 images	Calculated KW from 60 Images
124	121

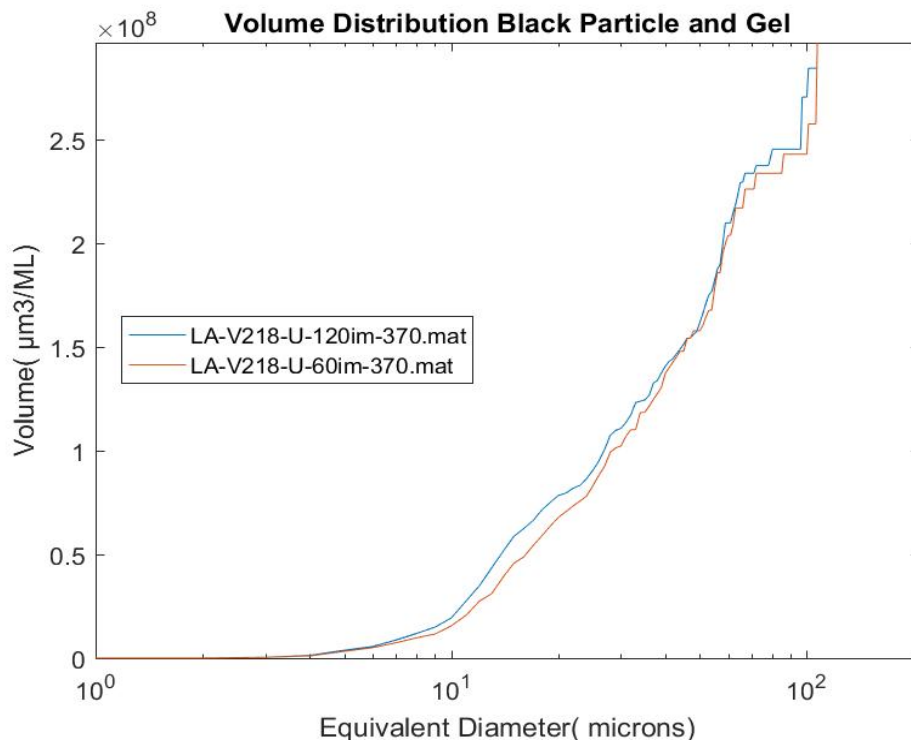


Figure 5.1: The reproducibility check for volume distribution of gels and black particles

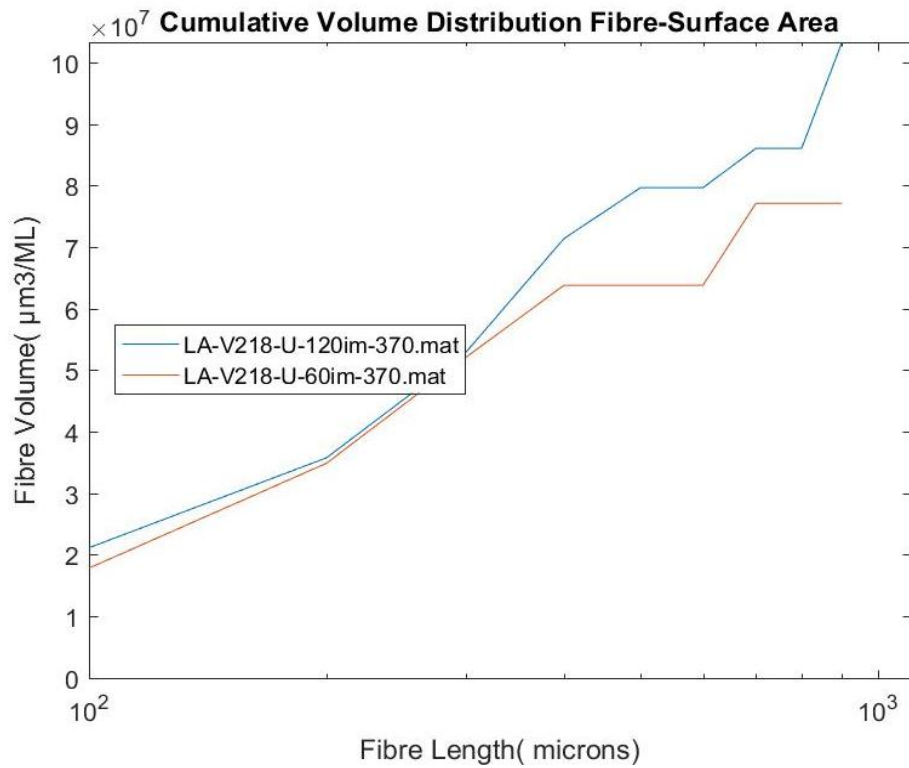


Figure 5.2: The reproducibility check for volume distribution of fibres

As seen from Table 5.2 the KW values calculated using the image analysis (details given in Section 4.4) also vary by a value of three which is acceptable for analysis. Figure 5.2 shows effect of number of samples images on volume integral, and indicates approximately 25 % deviation above size group above 500 micron. In view of reducing measurement uncertainty, final number of images to be processed per sample by the code was set to 200-250.

5.3 EFFECT OF BED THICKNESS ON CALCULATED KW VALUES

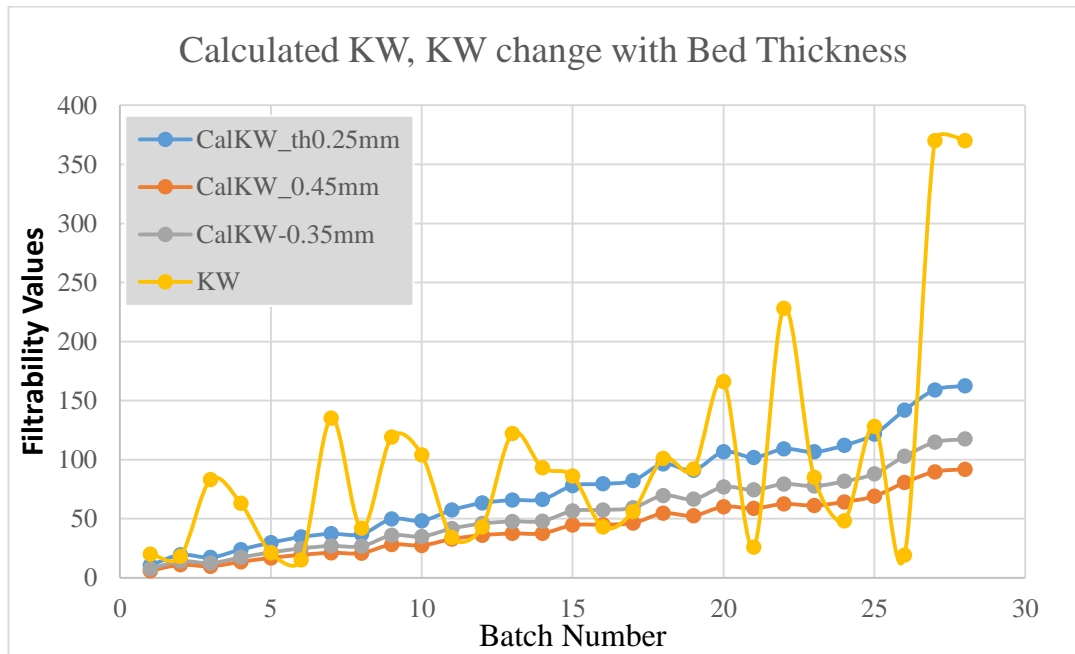


Figure 5.3: Calculated KW and KW variations with filter bed thickness

As the bed thickness of the filter bed of cotton mesh supported on poplin cloth and metallic wire gauge which gets compressed under the weight of viscose for filtration and the differential pressure applied is also seen to impact the filterability values as shown in Figure 5.3. The figure shows the variation of calculated KW for minute variation of bed thickness in range of 0.25mm to 0.45mm for 28 batches of different viscose samples. The x-axis is the batch number. The batches are arranged in ascending order of total volume of impurity per ml of viscose, that is batch 1 is having the lowest volume of undissolved particles per ml of viscose and vice versa. The graph shows that the measured KW values for 50% of the batches lie within the calculated KW values.

5.4 EFFECT OF BED POROSITY ON CALCULATED KW VALUES

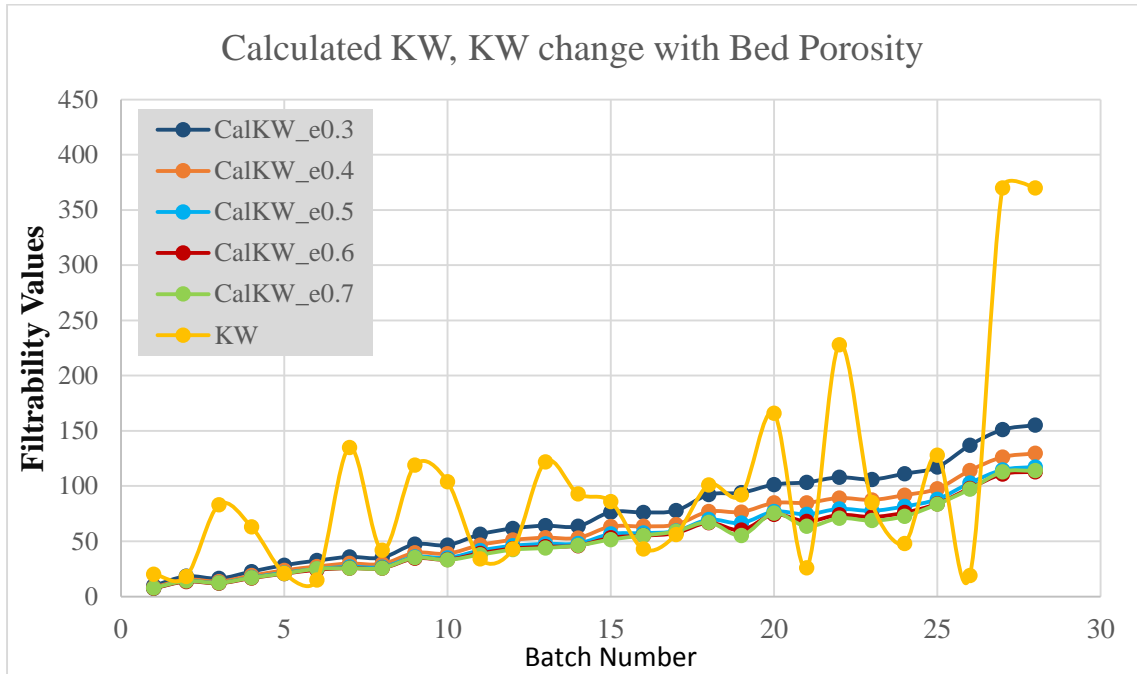


Figure 5.4: Calculated KW and KW variations with filter bed porosity

The cotton mesh filter bed does not have a well-defined porosity. As the initial bed porosity is another parameter input which is used in calculating KW values, it becomes important to check its effect on calculated KW. The bed thickness was kept constant at 0.35mm and the porosity was varied from 0.3 to 0.7. Again the batches have been arranged in increasing order of their total volume of impurity per ml of viscose. 50% of the batches shown in Figure 5.4 lie within the coincidence range of calculated KW and KW. The effect of porosity becomes more pronounced as volume of impurities per ml of viscose increases.

5.5 PARTICLE DISTRIBUTIONS from IMAGE ANALYSIS and KW

The focus here is on black particles and fibres. The changes in volume and number distributions of these two segments are depicted with the KW values. The batches are classified depending on their KW values and the plots show the trend of change in number and volume distributions in figures 5.5.1 and 5.5.2. The batch to batch comparison is done with these plots. As the plots of volume distributions are more informative for filterability values obtained using meshed cotton cloth, the number distribution plots are useful when a synthetic membrane of uniform pore size is used for filtration of viscose.

These plots provide a basis of comparisons with other particle size analyzing equipment such as Beckman Coulter or Laser Particle analyzers.

The binning for black particles has been done in integer values of equivalent diameter ranging from 1 to maximum equivalent diameter for the batches analyzed. The binning for fibre length is for 100 micron, that is the fibre lengths from 1-100 micron lie in bin 1 and from 100-200 micron lie in bin 2 as seen in figure 5.5.1 and 5.5.2.

Black particle volume distribution in figure 5.5.1 depicts the range of their existence in viscose analyzed. The graph for batch V255 however also helps us to know that some external particle could have been detected as the graph shoots at the end. For analysis the shoot up part for such batches can be neglected and the cumulative volume per mL can be taken as that at the previous equivalent diameter. The other batches show lower numbers of black particle volume per mL.

Similarly, fibre volume distributions in figure 5.5.1 depict the range of volume/mL for fibres. The final cumulative volume/mL obtained at fibre length of 1100 microns shows the trend of increasing with increase in KW values.

The number distributions shown in figure 5.5.2 add more information for comparing particle distributions. As the batch V244 is having more fibre segments above fibre length of 200 microns and lower number of fibres below that it is having higher KW where black particle contribution to KW is less. Batch V256 and VE 216 also have higher KW where the fibre contribution is as high as in V244, but black particle contribution is more.

5.6 CORRELATIONS OF PARTICLE SIZE DISTRIBUTIONS WITH KW

A preliminary look at Figure 5.5.1 depicts that KW and total volume/mL which is a summation of volume/mL of all segments of impurities (fibres, black particles and gels) over all particle sizes has no correlation with KW. However, as the polynomial of degree 4 is tried to fit, we get a good fit with R-square value of 0.602. The polynomial fit justifies the physical phenomenon.

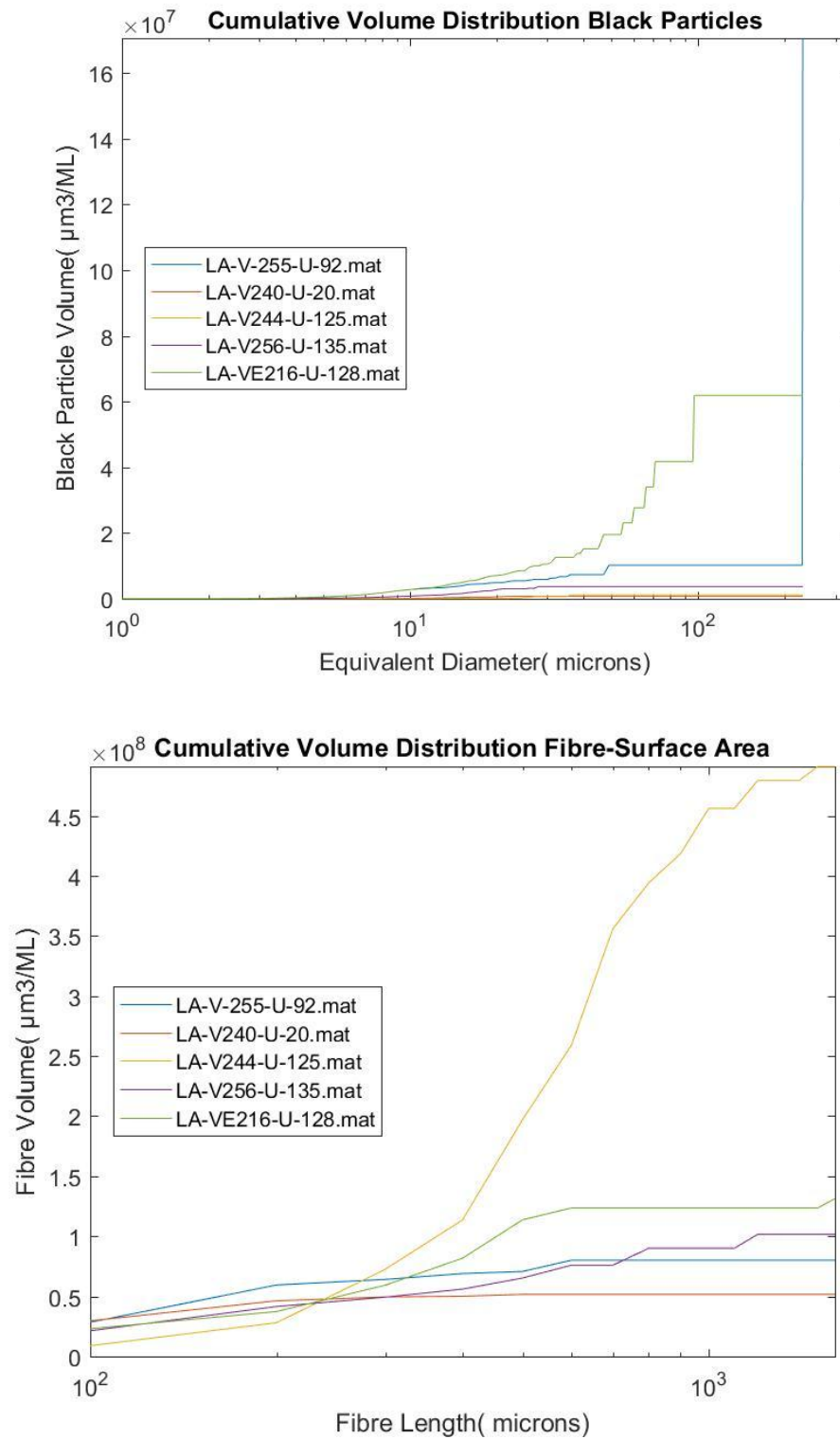


Figure 5.5.1: Cumulative Volume Distributions for fibres and black particles for batches with different KW values

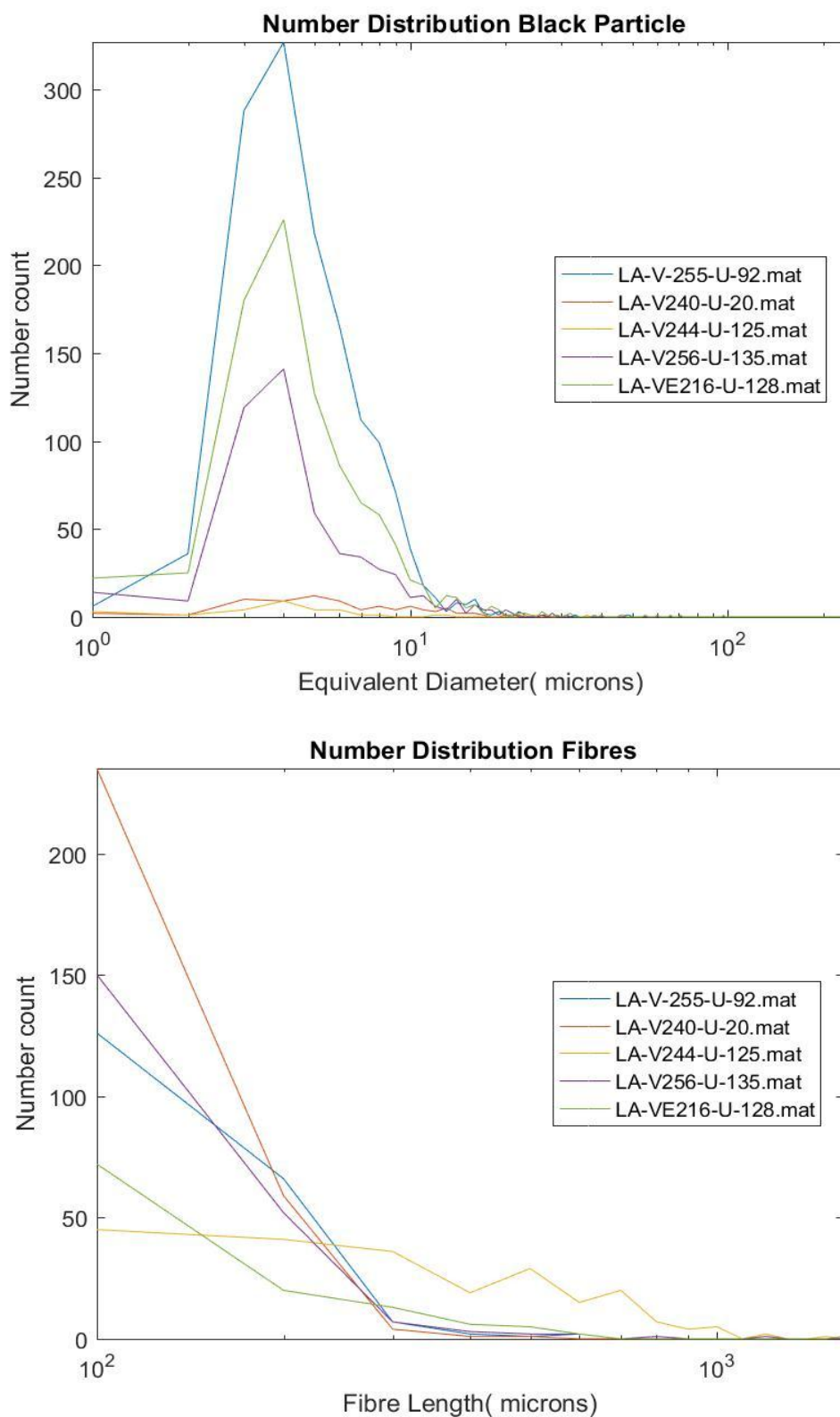


Figure 5.5.2: Cumulative Number Distributions for fibres and black particles for batches with different KW values

HYPOTHESIS 1: The contribution to KW is a function of volume of gels, fibres and black particles as well as the total volume of impurities. This implies that the same KW value can be achieved by different proportions of fibres, black particles and gels in same total volume of impurities. This could lead to six different combinations of volume fractions of the three types of impurities at a given total volume of impurities per mL of viscose. The degree four polynomial fit shown in Figure 5.6.1 is a representation of four different combinations. A polynomial of degree six will lead to a better fit as all the six combinations of volume/mL of gels, fibres and black particles will be taken into account that could give the same filtrability values. The extrapolation of polynomial of Figure 5.6.1 is expected to have another minima as the total volume/mL increases.

Figure 5.6.2 highlights this fact as with addition of batch of viscose with higher total volume/mL of impurities we see the polynomial getting towards another minima. The fit gives R-square of 0.453. The polynomial is expected to pass through the KW values of 370 to get a more appropriate fit. But the point could be an outlier also. At this point, more data is required to confidently say which outliers are and which are showing the trend different from that expected.

Also, the behavior of black particles with the filter paper will differ from that of gels and fibres with filter paper. While black particles larger than the pore size of filter cloth can lead to complete blocking of volume of filter cloth under it whereas the fibres and gels tend due gradually foul the filter cloth volume without crating much choking at the surface. With the viscose prepared at pilot scale plant of viscose the volume of black particle per mL of viscose is of range $8 \cdot 10^6$ - $5 \cdot 10^7$ and volume of fibres per mL of viscose is of range $7 \cdot 10^7$ - $5 \cdot 10^8$. The fibres thus contribute more to the KW and the further increase in their volume fraction will lead to much higher KW (Figure 5.6.3).

The sum of volume per mL for fibres and gels with KW values is done with logarithmic fit. The exponential fit is equally good and both have R-square of 0.367 (the inverse relation is a required fit as shown in Figure 5.6.1). Intuitively, the possibility is that within each maxima sandwiched between two minimas of the polynomial of degree six there exists an exponential/logarithmic fit of volume/mL of fibres and gels with KW

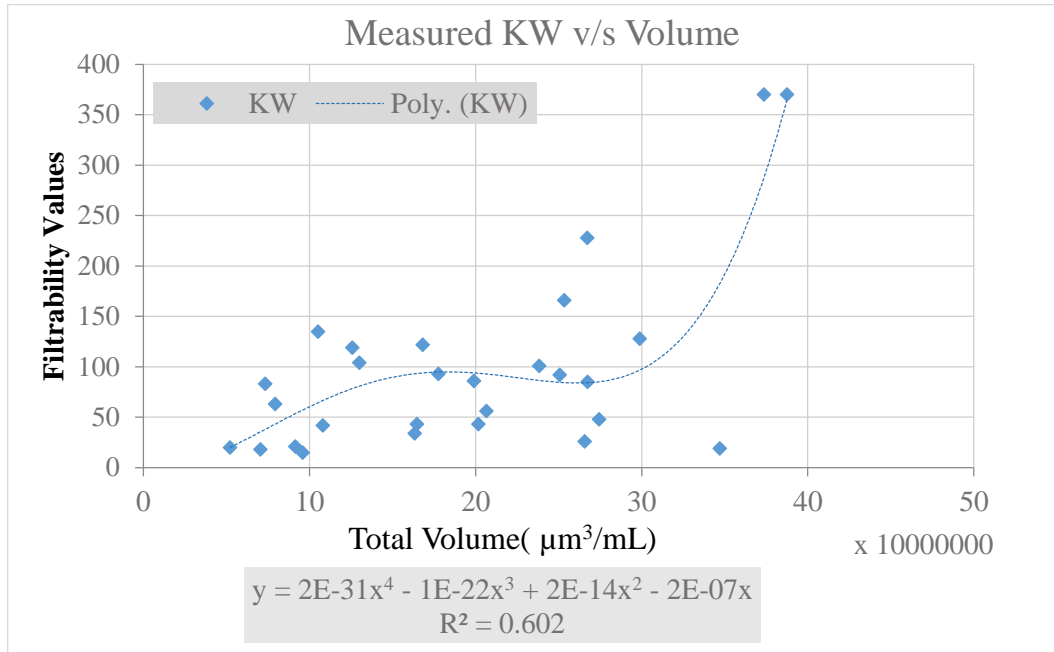


Figure 5.6.1: The correlation of KW with Total Particle Volume/mL from Image Analysis

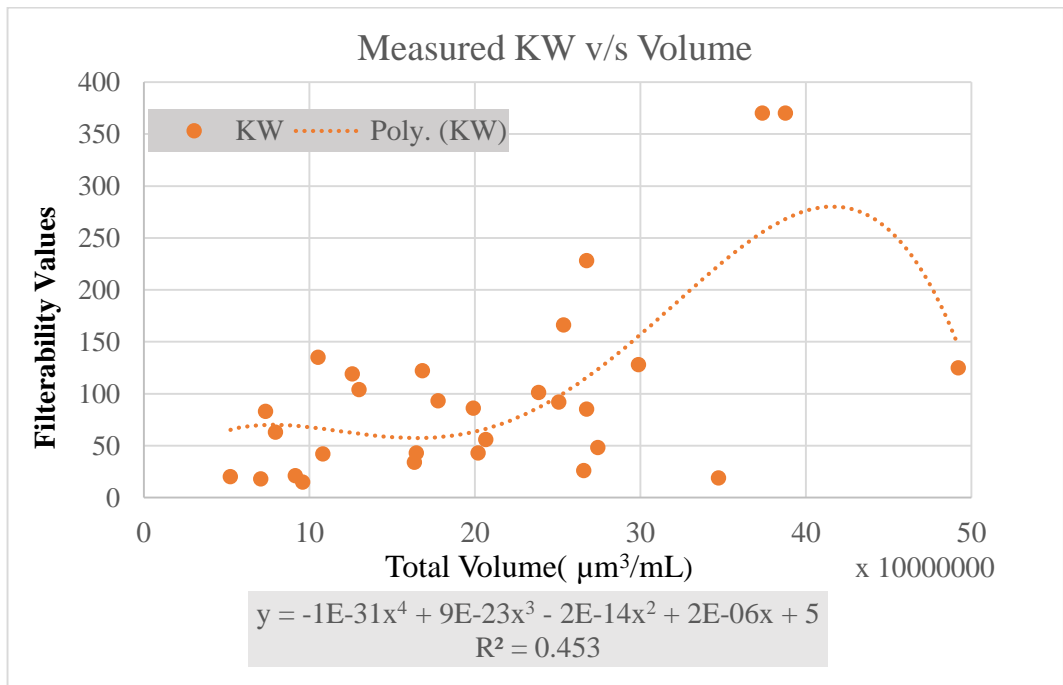


Figure 5.6.2: The correlation of KW with Total Particle Volume/mL from Image Analysis with one more data point addition

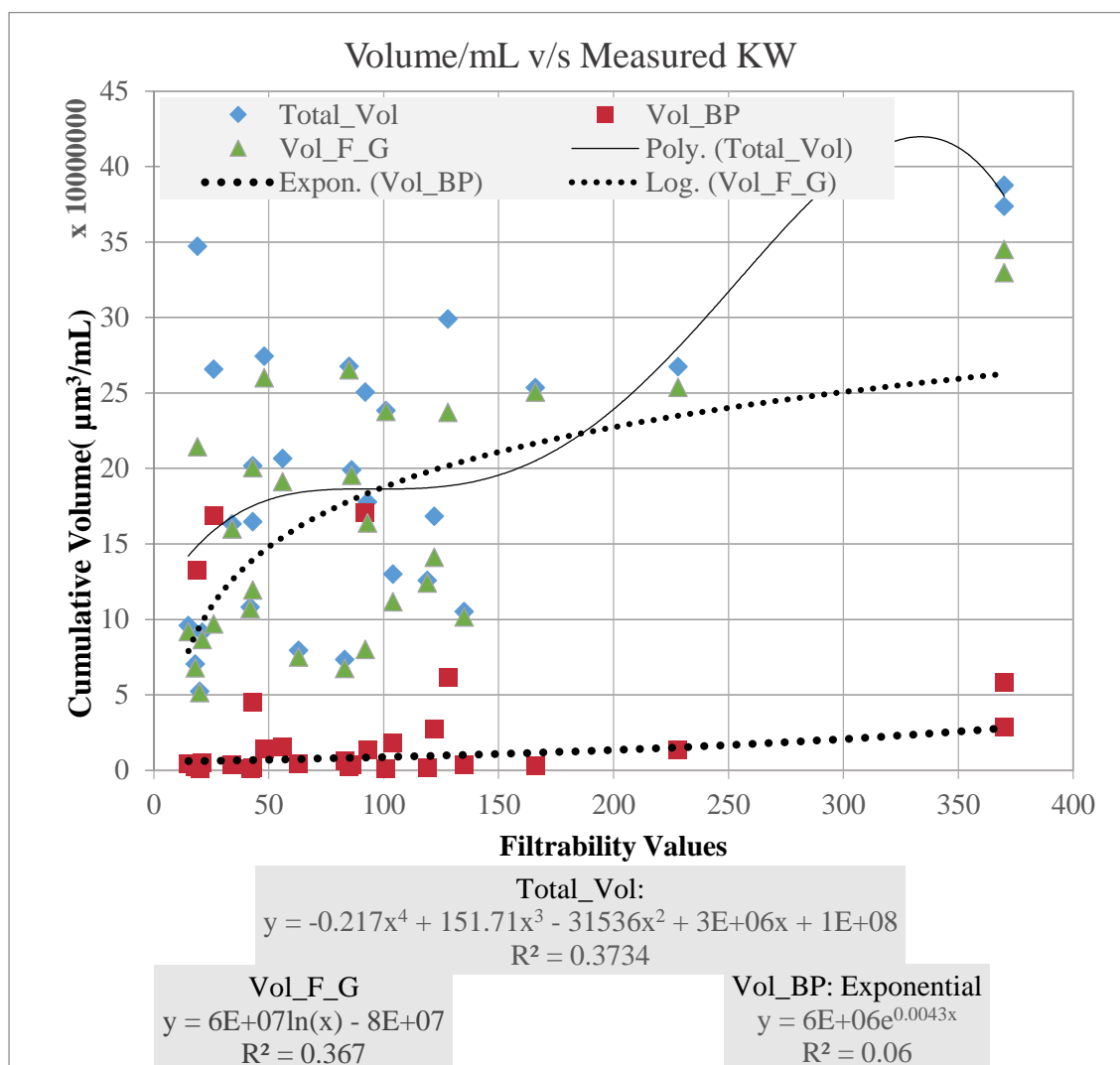


Figure 5.6.3: The correlation of KW with Total Particle Volume (Total_Vol), sum of Fibre and Gel Volume (Vol_F_G), Black Particle Volume (Vol_BP) from Image Analysis

having R-square greater than 0.60. The black particles follow a linear or exponential trend while exponential fit is a better fit as shown in Figure 5.6.3.

HYPOTHESIS 2: Another hypothesis is that both total volume of impurities per mL of viscose and sum of fibre and gels volume per mL of viscose follow power law trend while the black particle volume per mL of viscose gives an exponential trend as shown in figure 5.6.4. Here, the particle size distribution of three batches that were showing higher black particle volume as seen from figure 5.6.3 are reduced to lower volume of black particles per mL of viscose after manually investigating their particle size distribution curves from MATLAB. The sharp rise of cumulative volume per mL at the

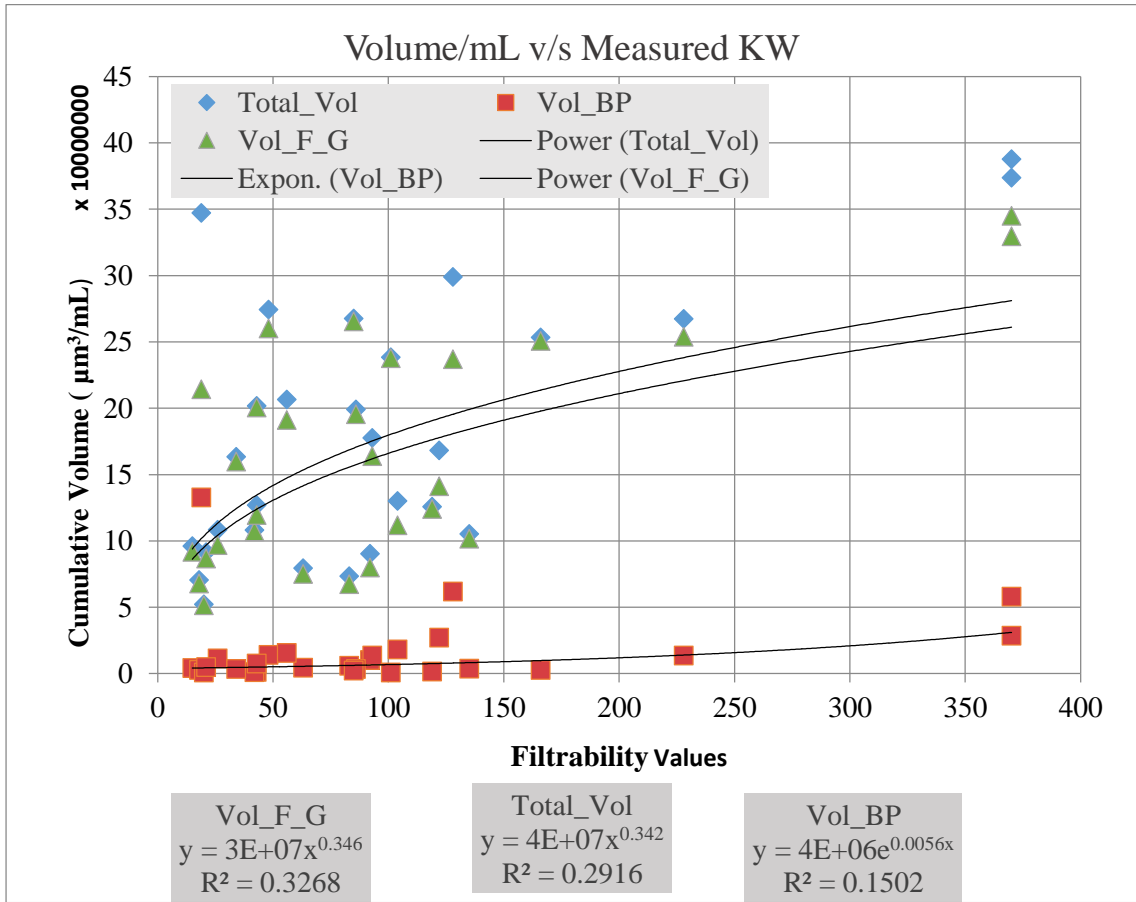


Figure 5.6.4: Modified correlation of KW with Total Particle Volume (Total_Vol), sum of Fibre and Gel Volume (Vol_F_G), Black Particle Volume (Vol_BP) from Image Analysis

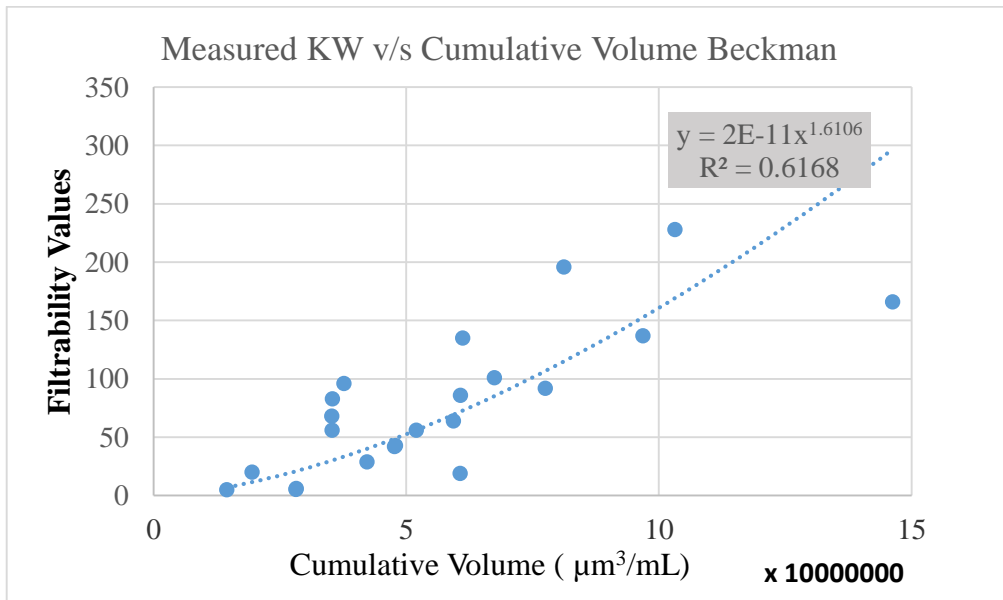


Figure 5.7.1: The correlation of KW with Cumulative Volume (µm³/mL) from Beckman Coulter

highest equivalent diameter of particle seen in graph has been reduced to its previous maximum value before the shoot up.

5.7 PARTICLE SIZE DISTRIBUTIONS FROM BECKMAN and KW

In Beckman Coulter we use 1% (w/w) sample of viscose made in 0.4% NaOH to analyze the particle size distributions. The graphs obtained are thus at for dilute viscose.

Figure 5.7.1 shows a power law fit of cumulative volume from Beckman Coulter with KW values having a R-square of 0.6168. Beckman Coulter does not account for fibre volume. An uncertainty of gel volume being reported by Beckman Coulter is also there.

Figure 5.7.2 shows the plots of various batches of viscose analyzed with Beckman Coulter. The batches V233, V234, V230 have particle size range of 18×10^4 - 33×10^4 $\mu\text{m}^3/\text{mL}$ and a KW in range of 15-19 (Table 5.7). The batch V229 has a KW of 42 and cumulative particle volume nearly 49×10^4 $\mu\text{m}^3/\text{mL}$. The plots show the trend of increasing cumulative volume per mL with increasing KW. The particle size distributions for higher KW values of 100-135 are given in figure 5.8.1 and batch details in Table 5.7.

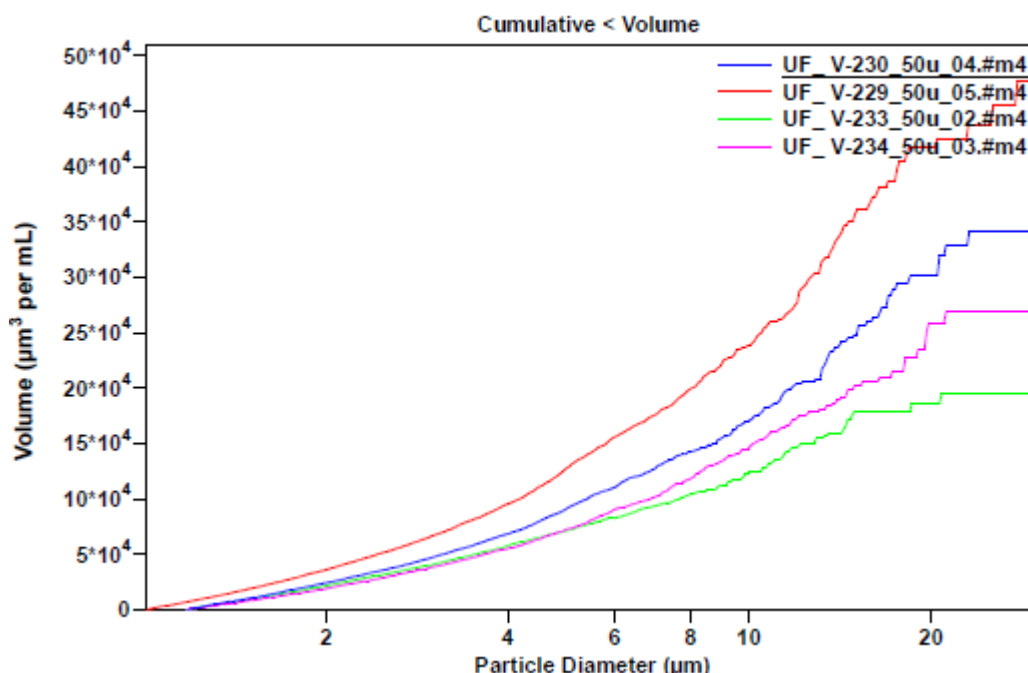


Figure 5.7.2: Particle Size Distribution from Beckman Coulter for 1% viscose sample

Table 5.7: Viscose Batch Details

Batch	KW	BF (in seconds)	Batch	KW	BF (in seconds)
V229	42	75	V253	101	91
V230	19	68	V254	83	85
V234	15	68	V255	92	88
V233	19	113	V256	135	120

5.8 A COMPARISION OF UNACCOUNTED INFORMATION IN BECKMAN WITH IMAGING

The particle size distribution from Beckman and Imaging is shown for batches V254, V255, V256. Batch V255 is standard batch for pulp A. Batch V256 is 50:50 of pulp A and pulp B while batch V254 is 20:80 of pulp B and pulp A respectively. The KW of the batches are given in Table 5.7. The batch V255 has been done at 2 concentrations of 0.5% and 1% viscose each in 0.4% NaOH figure 5.8.1 which is the cumulative volume from Beckman is also in trend with KW, however batch V255 has KW of 101 and but the curve for 1% viscose (indicated in legend on graph) it lies above V256 which has KW of 135 (figure 5.8.1). The imaging results however do not show any trend for black particles (figure 5.8.2) but for fibres the trend of decreasing cumulative volume per mL with decreasing KW is seen in figure 5.8.3. The imaging provides detailed information and helps us to know that the standard batch for pulp A and 20:50 batch with pulp B have same KW range of 83-92 and show the similar fibre volume distribution curve pattern (figure 5.8.3). Batch of pulp A and pulp B in 50:50 ratio shows higher KW of range 135-170 (checked with other batches) has a different fibre pattern where we see longer fibre length in viscose of this batch and thus higher volume of fibres per mL at those lengths. This information is not shown by Beckman Coulter analysis. Hence, imaging techniques provided useful information not provided by other particle size analyzing techniques for viscose samples without any need for dilution.

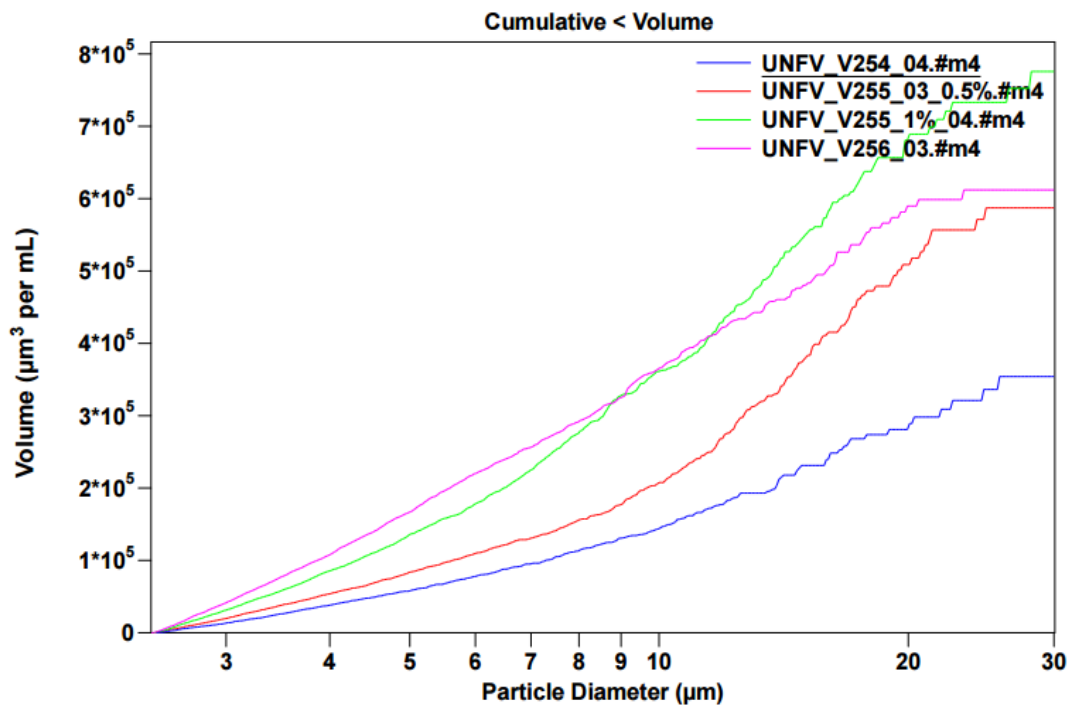


Figure 5.8.1: Particle Size Distribution from Beckman Coulter for 1% viscose sample for comparison to Imaging Results

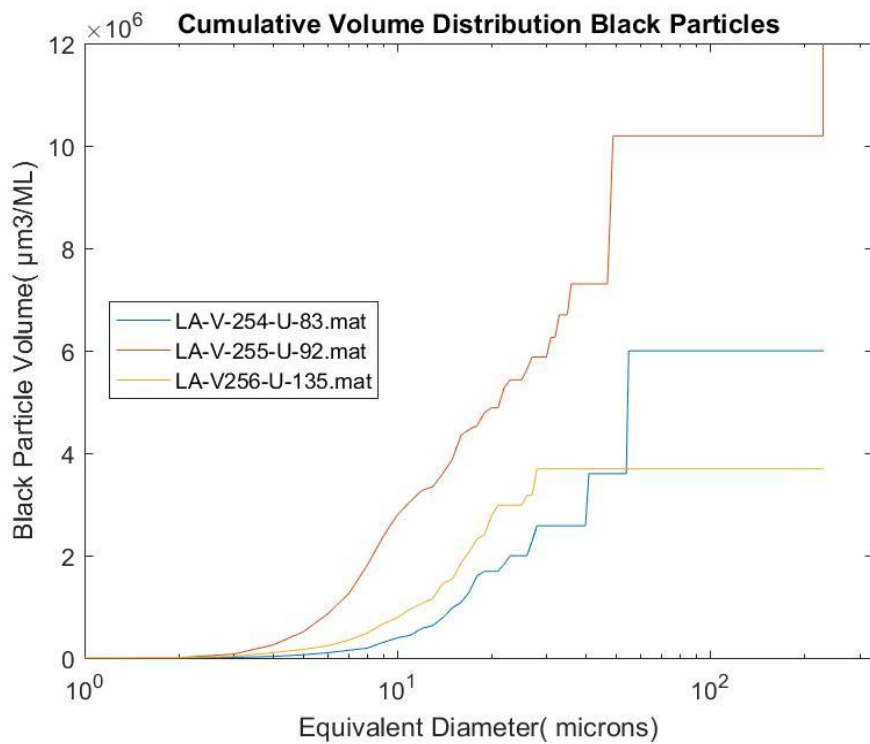


Figure 5.8.2: Black Particle Distribution from Imaging for comparison to Beckman Results

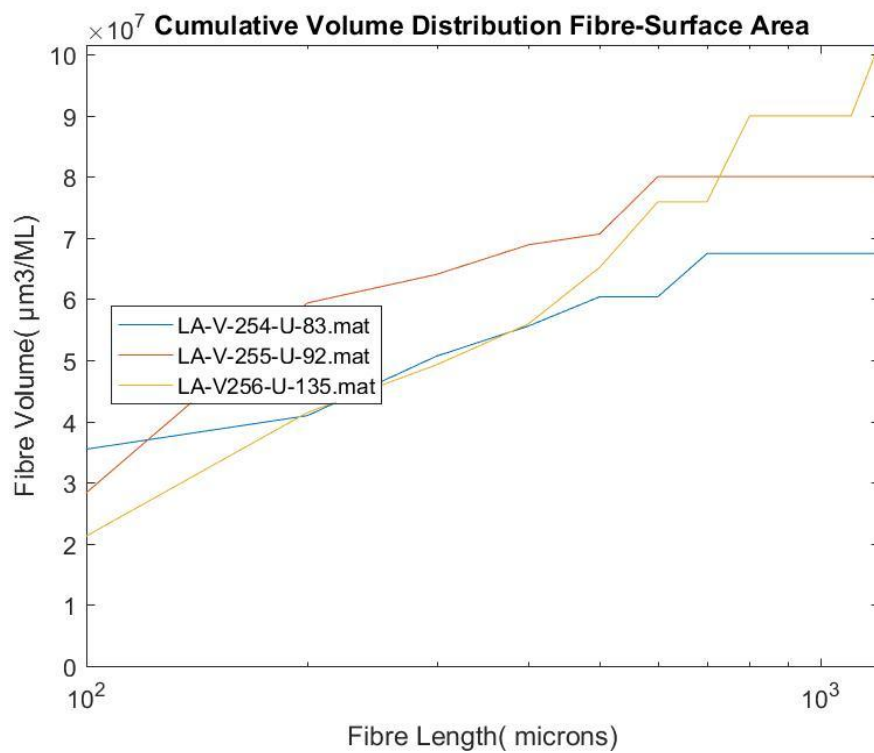


Figure 5.8.3: Fibre Distribution from Imaging for comparison to Beckman Results

CHAPTER 6

CONCLUSION

In the present work, impurities in the viscose have been analyzed and quantified using two methods, namely, Beckman coulter counter and imaging. Main aim of the thesis has been to identify different types of impurities and understand their effect on filterability constant of the viscose.

The exact quantification of particles in viscose is a challenging task for two reasons. First, the Beckman coulter, light scattering equipments and laser techniques give only a blurred insight into the distribution of microscopic particles in viscose. These techniques do not help to know the changes in viscose filterability is caused by which segment of undissolved particles that is fibres, gels, knots or black particles. The undissolved fibre sizing is not available in them. Second, the viscose itself is in a dynamic state. The particle distribution keeps changing accounted to agglomeration of gels with time and dispersion and breaking into smaller particle sizes upon mixing.

The imaging techniques provide a useful tool to quantify particles in microscopic range with the viscose flowing through the flowcell. The undissolved fibres (fibre knots, swollen and not swollen fibres), transparent/ translucent gels and black particles can be studied separately to check the effect of operational parameters such as CS₂ concentration, temperature and pressure variations at mercerization, xanthation and dissolution, change of pulp and additive addition on each of these section of particles comprehensively.

Experiments with different viscose batches and comparison of particle size distributions from Beckman Coulter and image processing in MATLAB have been done. The cumulative particle volume per mL of viscose obtained from Beckman shows a power law fit with R-square of 0.61. However, when looked at black particle volume distribution in image processing the power law fit gives a lower R-square of 0.15. The cause can be the addition of foreign impurities with dye solution. This aspect can be eliminated by imaging undyed viscose and getting black particle distributions from that.

The expected value of R-square for power law fit to fibre volume distribution per mL from imaging to KW was above 0.70. However, that gives R-square of 0.25. The logarithmic fit was found to be better here with R-square of 0.36 and requires more experimentation and data inputs. The Beckman coulter results do not show the fibre volume distribution which can be analyzed with image processing code for dyed and undyed viscose samples.

The issue of key importance is that translucent particles need to be detected effectively through image processing codes else it may lead to substantial loss of information. These particles are visible as scintillating tiny dots skimming across the flowcell viscose as seen under the microscope. Work was done towards coloration of translucent particles with dyes such as Congo Red which has high affinity to cellulosic material and thus creating a contrast in the remaining viscose using another color dye such as Aniline blue. It was to help prevent loss of number of particles counted by imaging code in MATLAB and reduce the work at coding stage. Prior to use, the concentration of dye solutions used for viscose dope coloration has to be investigated to ensure proper mixing and prevent dye agglomeration and dye film formation. Dye solution should be added to viscose dope after filtration through 0.2 micron filters so as to prevent addition of foreign particles as impurities.

The results and techniques presented in this thesis can be carried forward to get particle size distributions of viscose after scrutinizing coloration of gels and other translucent impurities in the desired size range, or else the imaging code can be made robust to process and count the translucent impurities effectively along with easily detected fibres and black particles. Relations of particles size distributions to filterability values are dependent on filtration method, filter material and size, filtration time and model used for correlation.

REFERENCES

- A. Virezub, V. K. (1972). Variation of gel particle content of viscose during the ripening process.
- A.A Serkov, N. K. (1986). Effect of hemicellulose on the productivity of mercerizing units and viscose filterability. *Fibre Chemistry* , 364-366.
- A.I. Virezub, A. P. (1978). Viscose Filtration (Review). *Chemistry and Technology of Natural-Polymer Fibres* , 246-254.
- C. Ghidaglia, L. A. (1996). Transition in Particle Capture in deep bed filtration. *The American Physical Society* , 3028-3031.
- D.N Arkhangelskii, V. D. (1973). A method of determining viscose quality. 3.
- E. Treiber, H. N. (1963). New contributions to the state of solution of viscose. Gel particle counting and optical rotatory dispersion studies on viscose. *Journal of Polymer Science* , 20.
- Gonsalves, V. (1950). A critical investigation on the viscose filtration process. *Recueil* , 30.
- H. Schleicher, B. B. (1998). Investigations on the state of solution of viscose. *Lenzinger Berichte*, p. 5.
- J. Coulson, J. R. (1998). *Chemical Engineering, Volume 2*. Asian Books private Limited.
- K. Brandt, S. S. *Requirements to Eliminate Gel Particles in Different Processes*. Lenzing, Austria: LenzingTechnik.
- L.A.Rykova, V. B. (1991). Formation of secondary gel particles in viscose. *Fibre Chemistry* , 2.
- L.R. Parks, K. J. (1960). Number and Size Distribution of Particles in Cellulosic Solution. *Journal of Applied Polymer Science* , 7.
- N. Dhanachandra, K. M. (2015). Image Segmentation using K-means Clustering Algorithm. *Procedia Computer Science* , 764-771.
- N. Katagiri, E. I. (2016). Developments of Blocking Filtration model in membrane filtration. *KONA powder and Particle Journal* , 179-204.
- Sperling, L. (1963). Characterisation of small gels in viscose. *Journal of Applied Polymer* , 13.

Treiber, E. (1961). The state of solution of technical viscose. *Journal of Polymer Science*, 19.

MATLAB Documentation, <http://www.mathworks.com/>

Biovis Particles Plus, Particle Size Analysis Software, Expert Vision Labs, *Biovis*